New Configuration for GAIA

Technical Report **N. 61** - October 2001

D. Loreggia, D. Gardiol, M. Gai

Summary

1. Introduction

A new configuration for GAIA interferometer is presented. Optical design and performances are discussed for different Effective Focal Length (EFL) and Apertures Geometry.

Optical designs and analysis have been implemented with CODE V Software Package [5].

In some papers [1][2][4] the basic topics of the interferometer and the various steps of the project history are presented. In literature, the interferometric configuration for GAIA is named "Backup configuration" and is one of two different working modes, which have been studied in the past [1].

We limit our preliminary discussion of the working scheme, referring to the references for any widening.

GAIA collects light from two apertures that look at two different directions (lines of sight - LOS) at a base angle of about 1rad (54deg). These two portions of sky reach a beam combiner that reflects light to the primary mirrors of the interferometer. The optics are aligned in such a way that each field impinges on half mirror, as reported in following figures:

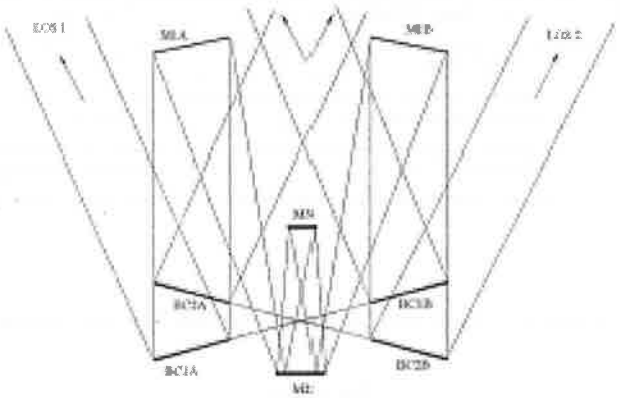

Fig. 1 Beam Combiner

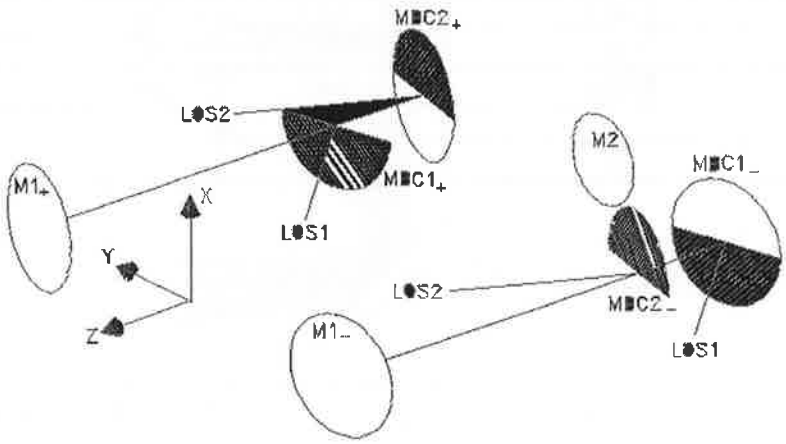

Fig. 2 Each sky part covers half of the primary mirrors

System works as a Fizeau interferometer with the primary mirrors M1 parts of a single surface.

These mirrors reflect light from targets to the secondary mirror M2 that focus it back along the optical axis. Now, light reaches a 45deg folded M3 (flat) that reflects focused light (M3 is not exactly at the M1+M2 focus) through M4 (conic). The latter re-focuses the beam back to another flat mirror M5 that deviates the light to the Focal Plane.

M2, M3, M4 and M5 are on the same plane, so to reach M5 light travels again in the M3 space and, for this reason it is necessary to have holes somewhere on the M3 surface.

The condition to have as low as possible spreading of light on M3, as seen by M4, is to optimise the design locating on M3 the exit pupil of the system.

The accepted scheme of the Backup Configuration for GAIA was designed in ALENIA – Aerospazio and is detailed in the Payload document [2].

The main features are summarized here:

Parameter	Value
Circular Aperture Diameter	0.65 m
Baseline	2.45 m
Effective focal length	40 m
Overall FOV	1.4 x 0.8 squared degrees

Dimensions and characteristics of the elements involved are summarised in the table:

Element	Radius of curvature [mm]	Conic constant	Aspheric terms	Thickness [mm]
M1	6378.8	-0.99	-	2785.6
M2	1141.7	-3.13	-	1332.8
M3	∞	-	-	933.5
M4	1392.8	-0.63	-	933.5 + 1098.2
M5	∞	-	-	1219.8
Focal Plane	∞	-	-	Best Focus

The layout of this configuration is:

09:56:08

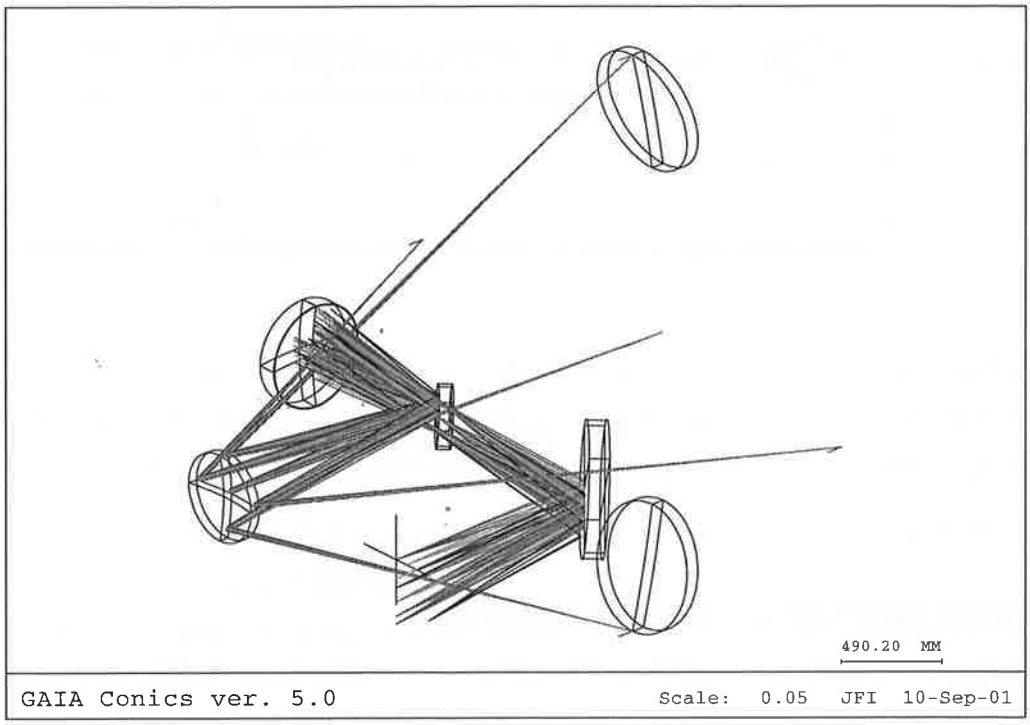

10:40:12

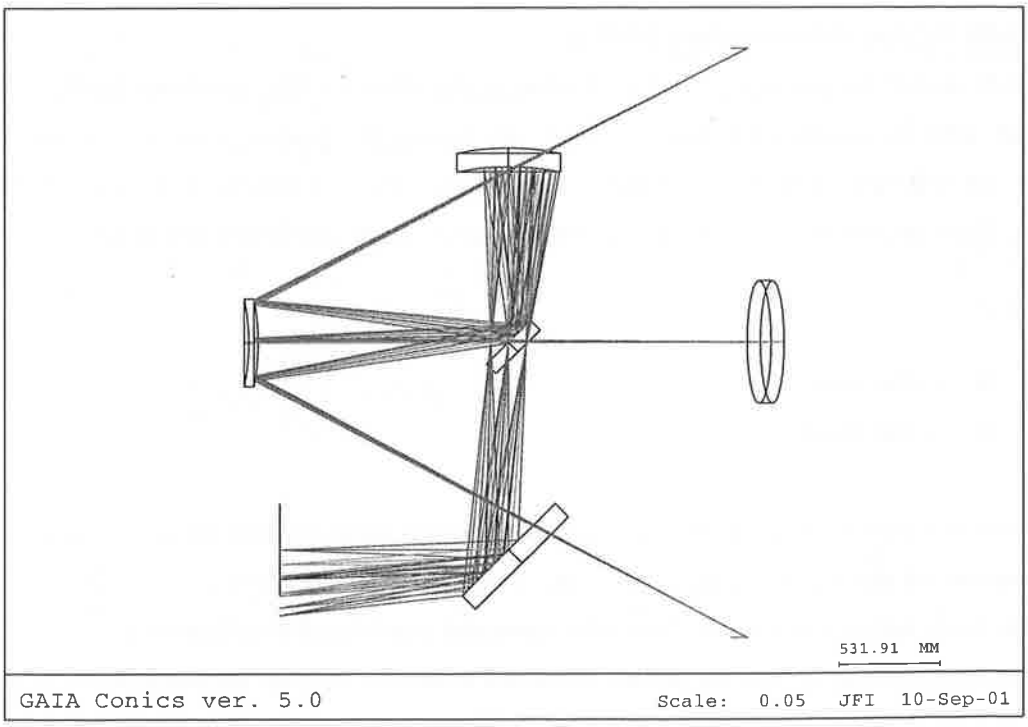

At the Focal Plane we have a light distribution, for the reference wavelength $\lambda = 750$ nm:

Airy Disk diameter	Number of fringes	Fringes period
154 mas 30 microns (on FP)	7	63 mas 12 microns (on FP)

To have sufficient resolution, we aim to sample each fringe with at least 3 pixels. Unfortunately with this configuration it should be necessary a CCD with pixels of 4 microns that is not available with current technologies, not only but the quantum efficiency for this case is of the order of 60% [1].

2. Optical Performances of the old configuration

Before discussing the new configuration and the gains in terms of optical performances we can get, it is useful to analyse the optical performances of the Backup configuration so to compare the effective improvements achievable. In particular, we will discuss the aberrations significance in the optimisation process for the new geometry of GAIA, considering the image quality in the nominal focal plane.

2.1 Tools for aberrations understanding

Every optical system acts on light introducing distortion on the wavefront profile that will never coincide with the gaussian reference sphere, which focuses in a precise point or in a completely shaped image, but will have some distorted shape, that will give rise to a blurred spot or a somehow distorted image. These imperfections are the *optical aberrations* and can be considered and described at two different levels:

- on the image plane
- on the wavefront.

In the first case we consider the deviations at the focal plane between the real focus of a ray and the nominal one (or paraxial focus) we could expect if the system was ideal.

This linear displacement is called ***ray aberration*** and is measured in **millimeters.**

In the second case instead, we call aberration the difference between the actual position of a wavefront point and the ideal one on the expected gaussian reference sphere.

This kind of aberration is named ***wavefront aberration*** and is usually expressed as fractions of **wavelength.**

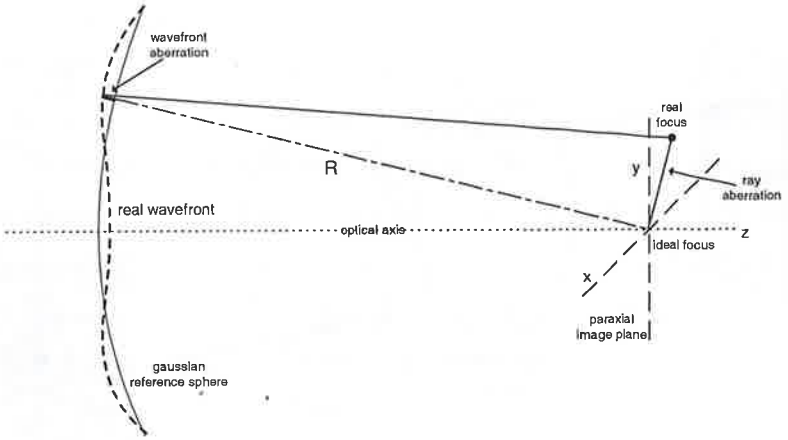

Fig. 3 Wavefront focusing geometrical scheme

In both cases the mathematical tool for expressing the optical perturbation introduced by the system itself is the representation as a polynomials series.

Usually the ***ray aberration*** is described in terms of Seidel polynomials that give a representation of the aberration considering only geometrical parameters of the system, as curvatures of optical surfaces, angle of incidence of the rays at the surfaces, coordinates of the ray-surfaces interceptions. Such a polynomial expansion can be carried to any order; third order or Seidel aberrations are the most significant.

CodeV third-order aberration analysis is based on classical aberration theory and image defects are expressed as polynomial expansions in object and pupil coordinates. They are calculated from paraxial data. In fact they can be computed using values derived from two paraxial ray traces, a marginal trace and a chief ray trace. The effect of each surface can be evaluated separately and then added.

Polynomial expansion for third-order aberrations is expressed as [3]:

$$Y_{j+1} - y_{j+1} = -\frac{1}{2n_j u_j}\left[\sum_{k=1}^{j} S_k \left(Y_1^2 + X_1^2\right)\frac{Y_1}{y_1^3} + \sum_{k=1}^{j} C_k \frac{\left(3Y_1^2 + X_1^2\right)}{y_1^2}\left(\frac{\bar{Y}_0}{\bar{y}_0}\right) + \sum_{k=1}^{j}\left(3A_k + F_k I^2\right)\frac{Y_1}{y_1}\left(\frac{\bar{Y}_0}{\bar{y}_0}\right)^2 + \right.$$
$$\left. + \sum_{k=1}^{j} D_k \left(\frac{\bar{Y}_0}{\bar{y}_0}\right)^3\right] + O(5)$$

$$X_{j+1} = -\frac{1}{2n_j u_j}\left[\sum_{k=1}^{j} S_k \left(Y_1^2 + X_1^2\right)\frac{X_1}{y_1^3} + \sum_{k=1}^{j} C_k \frac{\left(2Y_1 X_1\right)}{y_1^2}\left(\frac{\bar{Y}_0}{\bar{y}_0}\right) + \sum_{k=1}^{j}\left(A_k + F_k I^2\right)\frac{X_1}{y_1}\left(\frac{\bar{Y}_0}{\bar{y}_0}\right)^2\right] + O(5)$$

Where $I = \bar{y}_k n_k u_k - y_k n_k \bar{u}_k$ is the optical invariant, index k of the summatories identifies the surfaces of the optical system and the meaning of the other quantities is shown in figure.

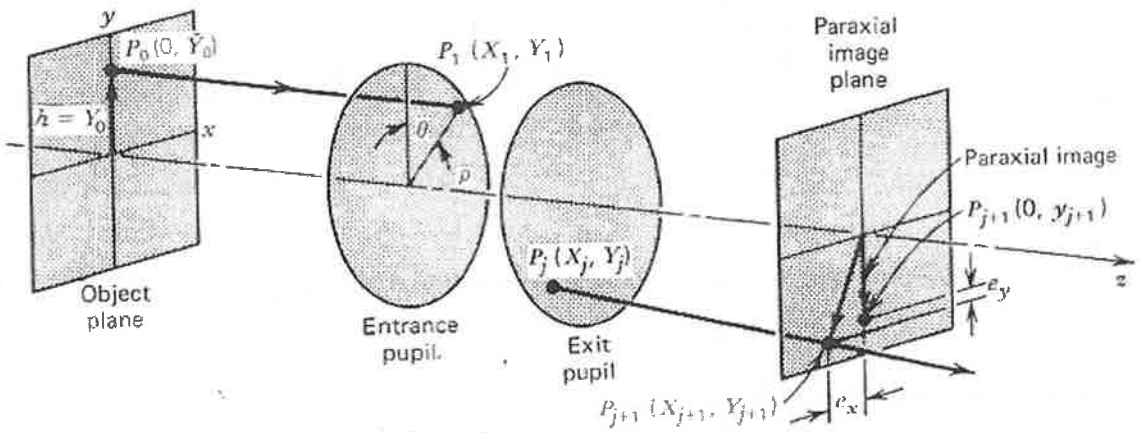

Fig.4 Ray tracing

Here a skew ray is launched from an object point $P_0(0,\bar{Y}_0)$ toward a point in the entrance pupil $P_1(X_1,Y_1)$. The ray intercept the paraxial image plane at $P_{j+1}(X_{j+1},Y_{j+1})$. The differences between the y- coordinates of the exact and paraxial traces (i.e. $Y_{j+1}-y_{j+1}, X_{j+1}-x_{j+1}\equiv X_{j+1}$) are the measure of the aberrations of the system. Each term in the polynomial can be identified with a particular type of aberration.

Corrispondence between Seidel terms and the aberration terms evaluated by CodeV is shown in table.

Aberration type	CodeV Acronym	Seidel corrispondence
Spherical	*SA*	$-\frac{1}{2n_j u_j}\sum_{k=1}^{j} S_k$
Tangential Coma	*TCO*	$-\frac{3}{2n_j u_j}\sum_{k=1}^{j} C_k$
Sagittal Coma	*SCO*	$\frac{1}{3}TCO = -\frac{1}{2n_j u_j}\sum_{k=1}^{j} C_k$
Tangential Astigmatism	*TAS*	$-\frac{1}{2n_j u_j}\sum_{k=1}^{j}\left[3A_k + F_k I^2\right]$
Sagittal Astigmatism	*SAS*	$-\frac{1}{2n_j u_j}\sum_{k=1}^{j}\left[A_k + F_k I^2\right]$
Petzval Blur	*PTB*	$-\frac{1}{2n_j u_j}\sum_{k=1}^{j} F_k$
Distortion	*DST*	$-\frac{1}{2n_j u_j}\sum_{k=1}^{j} D_k$

This formulation usually is exact for system with circular symmetry by the moment that the calculation takes into account the height of a single ray with regards to the optical axis and that extend the results validity to the whole beam by symmetry. For systems that don't fulfill this condition results must be considered as indicators of the overall behavior but not as exact values.

The system we are discussing is a particular case in which, if we consider each single aperture we haven't a symmetric system but if we consider the interferometer as a whole we can think it is.

If we call (X , Y) the projection on the reference frame *Oxy* of the ray aberration at the focal plane and R the radius of the reference sphere, ***Wave aberrations*** W(*x*,*y*) can be related to the ray aberrations by derivative as can be verified in [6][7]:

$$\frac{\partial W}{\partial x} = -\frac{X}{R} \qquad ; \qquad \frac{\partial W}{\partial y} = -\frac{Y}{R}$$

that means we can assume a Seidel polynomial expansion for the wavefront too, taking into account that the coefficients of each polynomial will be now *different* from the ray aberration case.

In order to define the wavefront completely, it is anyhow more convenient to think the aberration distribution as a function that can be integrated over the whole exit pupil of the system. By normalization we can consider a pupil as a unit circle and use a complete set of polynomials that are orthogonal over the interior of this circle.

Many sets of polynomial with this property can be constructed, but due to their invariance properties, the most used are the ***Zernike*** polynomials.

The algebraic form of this polynomial depends on the radius *r* of aperture over which is performed the integration (usually the exit pupil of the system) and on the azimuth angle φ referred to the vertical axis in the plane orthogonal to the propagation direction. One of the typical representations is:

$$W_{\text{Zernike}}(r,\varphi) = \sum_{n=0}^{G} \sum_{l=0}^{|l|\le n,\ (n-|l|)\text{ even}} Z_{nl} Z_n^l(r,\varphi)$$

Z_{nl} : Zernike coefficients

$$Z_n^l(r\cos\varphi, r\sin\varphi) = R_n^l(r)\cdot e^{il\varphi}$$

$$R_n^{\pm m}(r) = \sum_{s=0}^{\frac{n-m}{2}} (-1)^s \cdot \frac{(n-s)!}{s!\cdot\left(\frac{n+m}{2}-s\right)!\cdot\left(\frac{n-m}{2}-s\right)!} r^{n-2s}$$

$$G = 4;\ |l| \le n;\ (n-|l|)\text{ even};\ m = |l|$$

with n, m indices of the polynomial. The first term of this series, till the fourth order (do not forget that ray aberration is the derivative of wavefront aberration), gives respectively:

Aberration	Zernike polynomial	Image Effect	Aberration	Zernike polynomial	Image Effect
Z_1 Piston	1	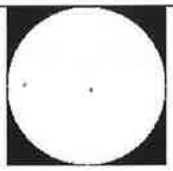	Z_6 Sagittal Astigmatism	R2 sin(2A)	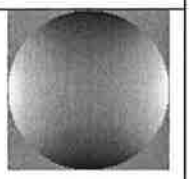
Z_2 Tangential Tilt	R cos(A)	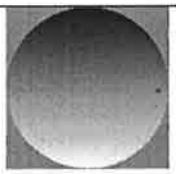	Z_7 Tangential Coma	(3R3 - 2R) cos(A)	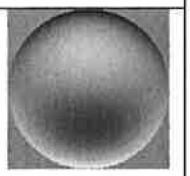
Z_3 Sagittal Tilt	R sin(A)	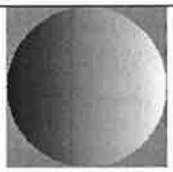	Z_8 Sagittal Coma	(3R3 - 2R) sin(A)	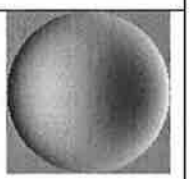
Z_4 Defocus	2R2 - 1	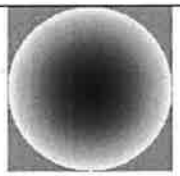	Z_9 Spherical	6R4 - 6*R2 + 1	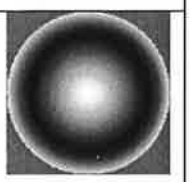
Z_5 Tangential Astigmatism	R2 cos(2A)				

The study of the wavefront aberrations of an optical system is aimed to determine the coefficients of the polynomials series, which give a quantitative estimation of each aberration contribution.

Any optimisation of such a system must be finalised to the minimisation of these coefficients trying to get performances as higher as possible.

2.2 GAIA Backup configuration optical behaviour

In this paragraph we apply these assumptions to the Backup configuration of GAIA. We report two tables that refers to the third order Seidel aberrations terms.

Assuming spherical symmetry, we can fix our attention only on a single direction for calculation, extending results validity to the whole wavefront. We consider the baseline direction that in our treatment is the Y-axis.

The fields we select for calculation are:

(0.0, 0.0) , (0.0 ; 0.1) , (0.0 , 0.2) , (0.0 , 0.3) , (0.0 , 0.4) , (0.0 , 0.5)

Each value reported in tables corresponds to the contribution to Seidel aberration of one of the outer marginal rays and represents the upper limit for aberrations.

Let's remark that we are speaking about the linear difference between the real focus point of the marginal ray and its correspondent paraxial focus and so the units are millimetres.

Ray aberration term	**Ray aberration value in mm between ideal and real focal points as function of the distance from the centre field**					
	0.0 deg	**0.1 deg**	**0.2 deg**	**0.3 deg**	**0.4 deg**	**0.5 deg**
Spherical			0.034			
Tan. coma	0.000	0.021	0.042	0.064	0.085	0.106
Tan. Astigmatism	0.000	0.003	0.011	0.025	0.044	0.069
Sag. Astigmatism	0.000	0.001	0.004	0.010	0.017	0.027
Petzval	0.000	0.000	0.001	0.002	0.004	0.006
Distortion	0.000	-0.005	-0.039	-0.132	-0.312	**-0.609**

The asymmetry of the system must be taken into account when we report the interferometric Point Spread Functions because points on the baseline direction and points on the corresponding orthogonal one will give rise to different photons distribution. As example, we consider the PSFs at points (0.0 , 0.4)deg, that is the external point on the high resolution positive direction, (0.7 , 0.0)deg, an external point on the low resolution positive direction, and (0.5 , 0.3)deg that is an external point in the first quadrant, fixed scaling by $\sqrt{2}$ the limits of FOV.

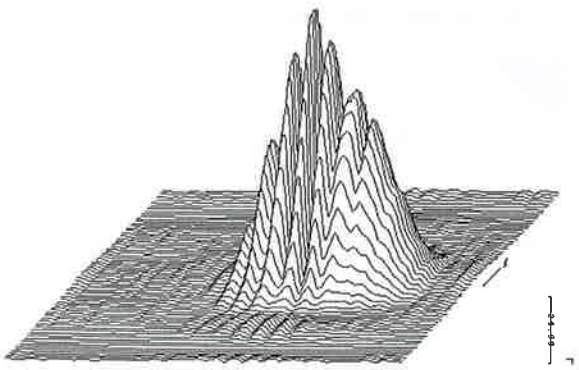

PSf at (0.0 , 0.4) deg

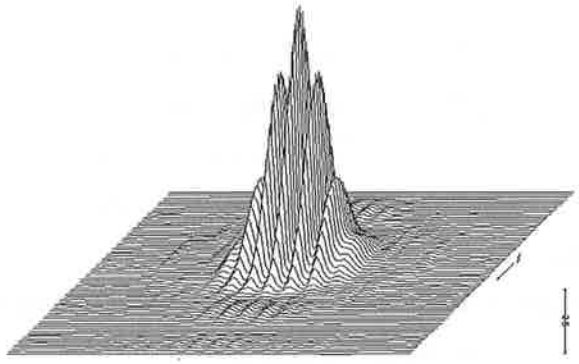

PSF at (0.7 , 0.0) deg

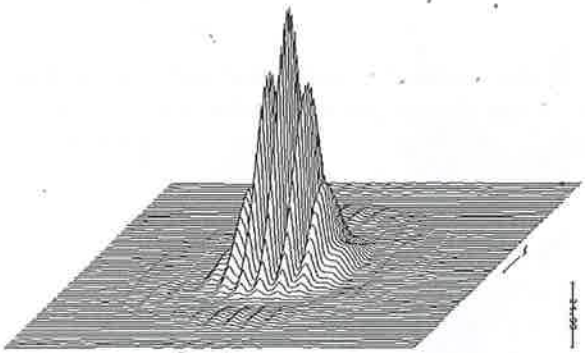

PSF at (0.5 , 0.3) deg

Performances are good even if in the first case (0.0 , 0.4), it is present a significant asymmetry on the PSF profile.

As further example we consider the PSF for the point (0.35 , 0.35)deg , that is one of the outermost point in the FOV we fix in the optimisation, as explained in the following.

This will let the reader to have a direct feedback of performances changes.

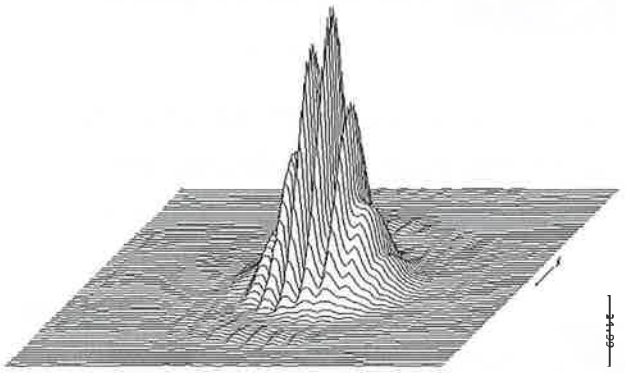

3. The new configuration

To improve the performances of the interferometer in terms of quantum efficiency and to overcome the problem related to the pixel size for the requested sampling, we studied a new configuration.

The Baseline configuration, the alternative one to the Backup Configuration as discussed in [1], fulfils the Focal Plane requirements reaching the target magnitude limit with an efficiency of about 90%.

The required pixel size in this case is 9 microns, a more realistic value. Such device can be used also for the interferometric configuration, provided that the scale factor of the system is reduced by an overall factor of about 2.25. This mean, by definition, that the focal length must be increased to 55m (instead of 40mm, the current value).

In this case, the requirement of sampling each fringe with 3 pixels, keeping about the same aperture dimension, forces to set a lower baseline. We fix B=1.4m.

The smaller baseline reduces the image resolution and therefore degrades the location performances. This means that we need to increase the SNR and recover the loss.

The simplest way is to modify the apertures shape, adopting square apertures instead of circular ones. This increases the amount of collected light of a factor $4/\pi$ with about the same space allocation, with the 41% of this gain going in the central lobe of the Airy Disk.

Besides the aperture dimension itself is increased from 0.65mm to 0.70mm, that means a further gain of a factor 1.2 in collecting area.

The configuration we studied has a total FOV smaller than the previous one and we are going to show its high performances everywhere in the field.

Parameter	Value
Square Aperture Side	0.70 m
Baseline	1.4 m
Effective focal length	55 m
Overall FOV	0.7 x 0.7 squared degrees

At the reference wavelength of 750 nm these parameters give:

Airy Disk diameter	Number of fringes	Fringes period
442 mas 118 microns (on FP)	4	110 mas 29 microns (on FP)

One of the most important task was to maximise the field dimension given by M2 on M3 at the reflection trough M4 and to minimise the pupil dimension given by M4 again on M3, so to hole only a small part of M3 to let light stream to M5. After several attempts a quite suitable optical scheme has been obtained:

Radius of Curvature (mm) Conic constant (K)		**Mirror Separation (mm)**	
M1	-6355.78	M1-M2	-2804.71
K1	-1.0		
M2	-869.20	M2-M3	2766.69
K2	-1.72		
M3	flat	M3-M4	573.18
M4	993.18	M4-M5	973.18*
K4	-0.74		
M5	flat	M5-FP	738.01

The distance M4-M5 is bounded to the imposed condition to have a distance between M3(back side)-M5 equal to an arbitrary fixed value of 40cm. This request rises up from the possibility to have M3 and M5 close enough to be assembled together.

The geometry of this system we got with CODEV, is:

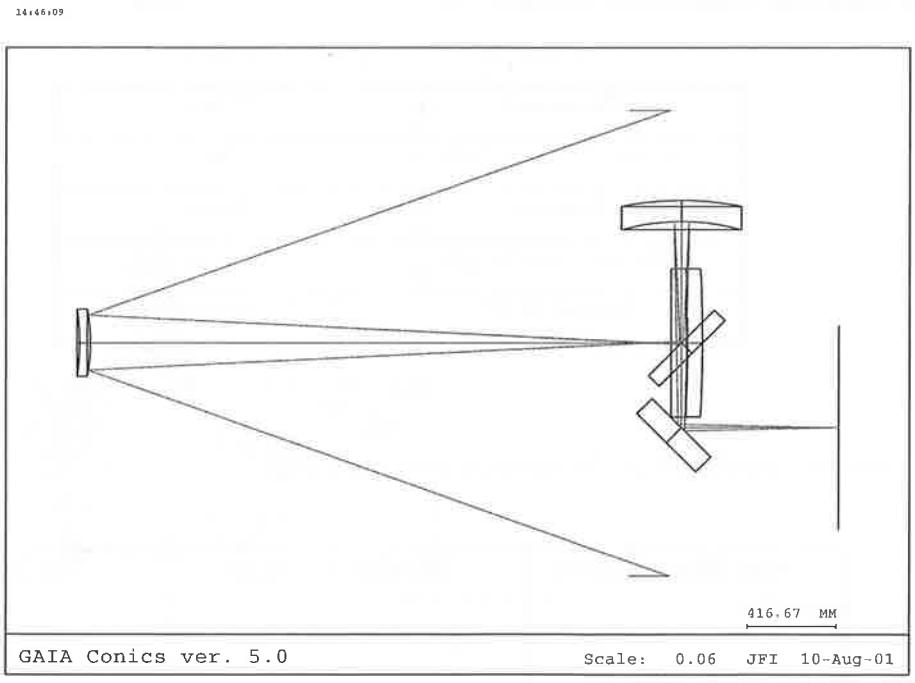

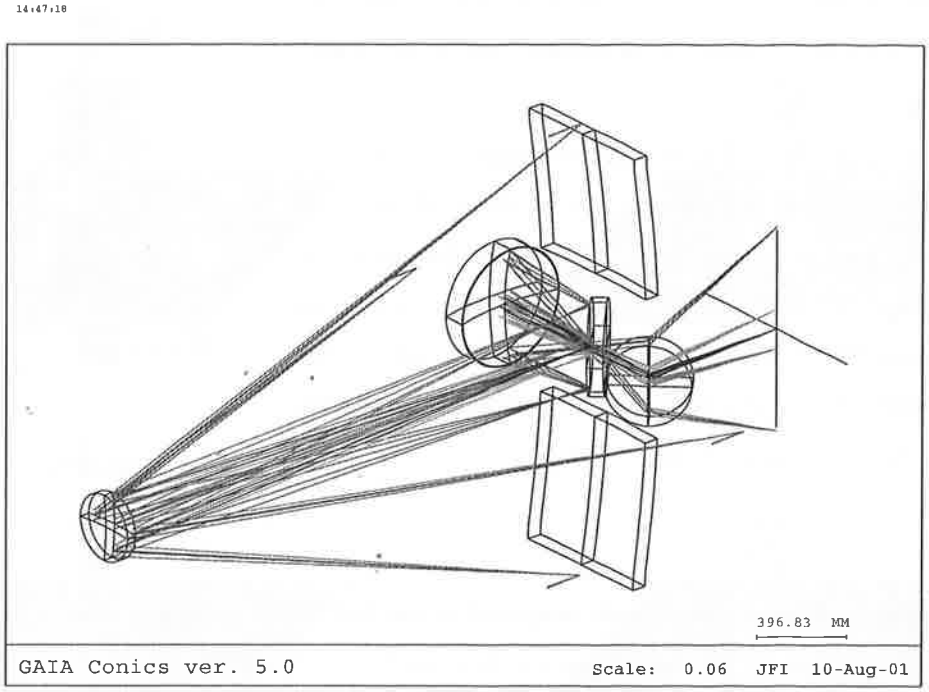

This configuration gives very good results if we look at the footprint analysis on M3

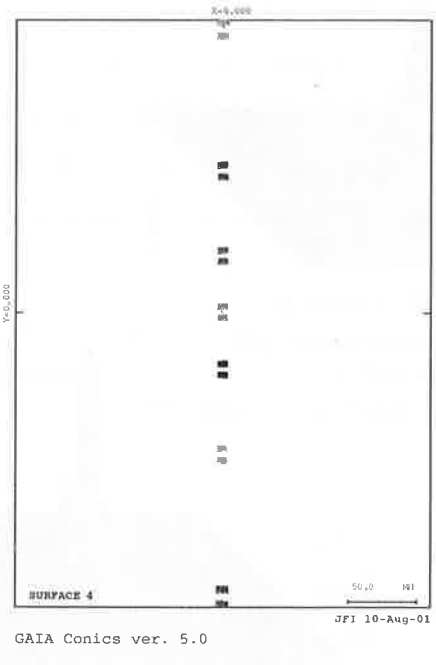

Footprint on M3 viewed from M2 *(field)*

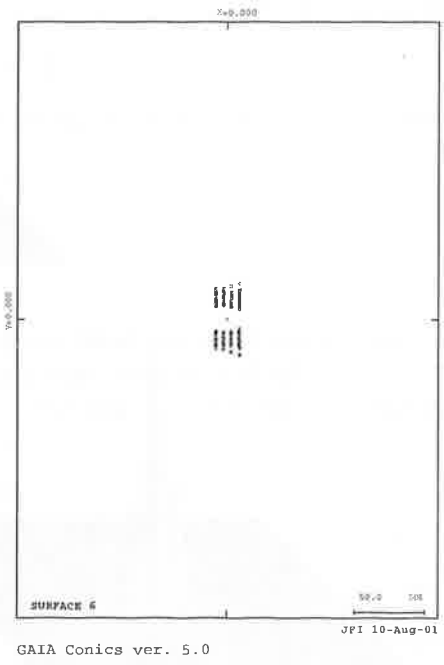

Footprint on M3 viewed from M4 (pupil)

In the picture, the footprint analysis at M3 viewed from M2 and from M4 respectively, is shown for fields ±0.50 , ±0.25 , ±0.10, 0.00 .

The reference scale (50mm) and the alignment of the field centres are the same and we can view in details the parts of mirror that must be cut out. Dashed lines mean the portion of the mirror that must be holed in order to enable the light to travel from M4 to M5. The central spot corresponds to the on-axis field (0.00 , 0.00) while the external ones corresponds to fields ±0.10 deg., respectively.

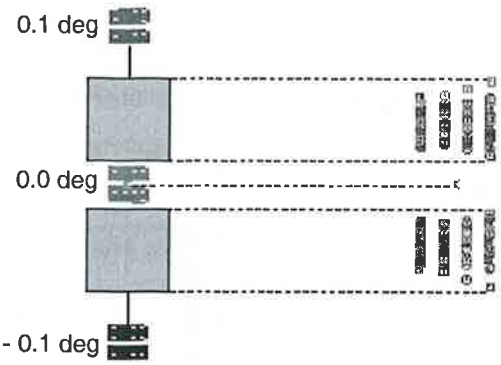

Area covered by the pupil on the M3

The vignetted area is very small compared to the full FOV, so we lose only a fraction of the total information close to the optical axis but not the central part of the field.

To taste the image quality for this configuration, in the following the PSF at different points of the covered field are reported, along the baseline direction (Y-axis, vertical).

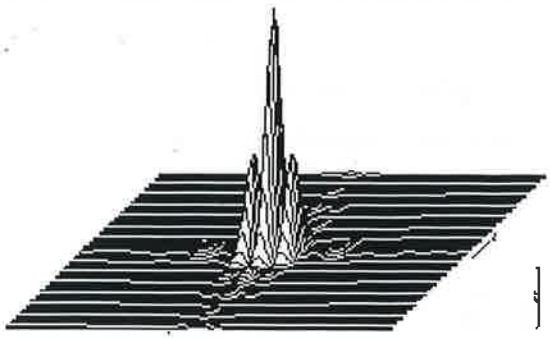

PSF at (0.00 , 0.00) deg

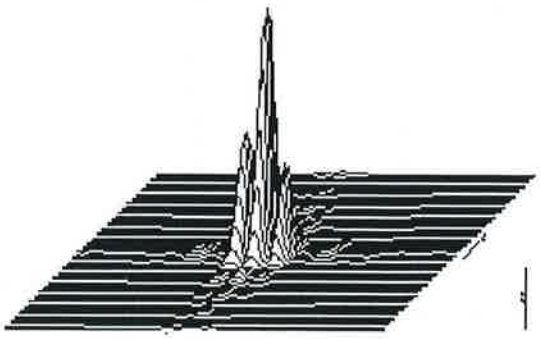

PF at (0.00 , -0.10) deg

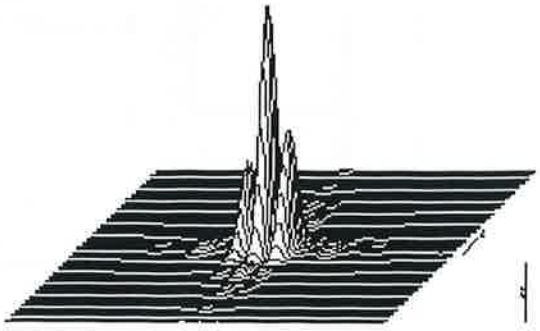

PSF at (0.00 , 0.10) deg

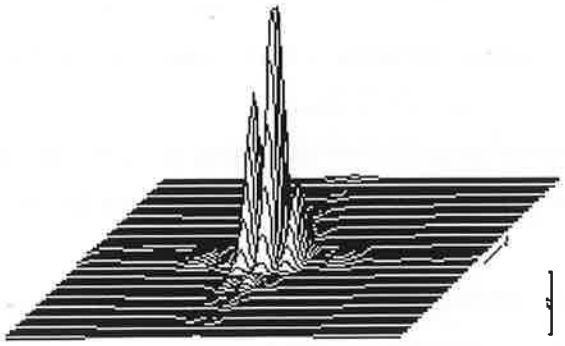

PSF at (0.00 , -0.25) deg

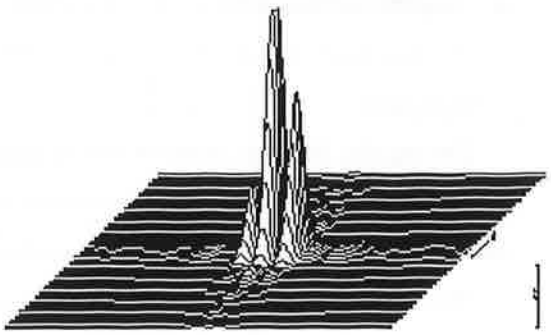

PSF at (0.00 , 0.25) deg

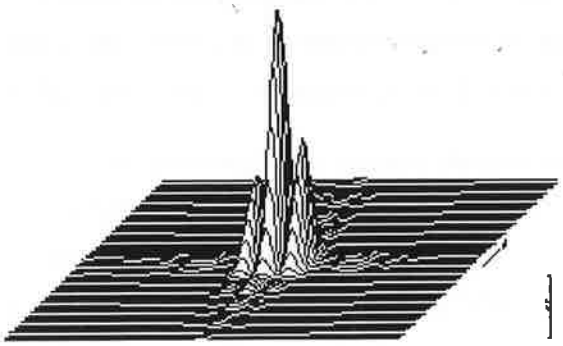

PSF at (0.00 , -0.50) deg

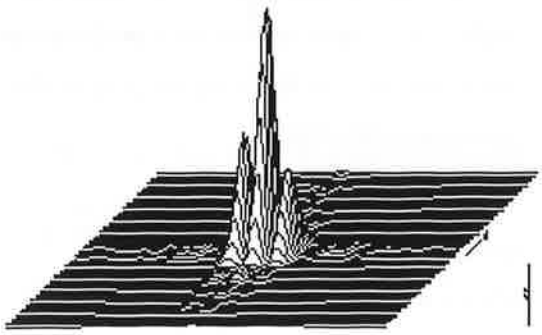

PSF at (0.00 , 0.50) deg

It can be noted that for fields ±0.25 the perturbation on the PSF profile is larger then for the PSF at ±0.50 and that there is an inversion of the asymmetry between ±0.50 and ±0.25-0.10.

Considering again the third order terms of the aberrations series along the baseline axis, we note that this behaviour could be due to distortion term that is significantly large.

The other terms seem to decrease.

Ray aberration term	**Ray aberration value in mm between ideal and real focal points as function of the distance from the centre field**					
	0.0 deg	**0.1 deg**	**0.2 deg**	**0.3 deg**	**0.4 deg**	**0.5 deg**
Spherical			0.006			
Tan. coma	0.000	0.015	0.031	0.046	0.061	0.076
Tan. Astigmatism	0.000	0.001	0.003	0.008	0.014	0.021
Sag. Astigmatism	0.000	-0.001	-0.006	-0.012	-0.022	-0.035
Petzval	0.000	-0.003	-0.010	-0.023	-0.040	-0.063
Distortion	0.000	-0.131	-1.050	-3.544	-8.401	**-16.409**

4. Optimisation with low distortion

At this point we try to optimize further this configuration, imposing a lower value for distortion contribution.

During the different fases of this optimization process we noted that the decreasing of distortion was somehow compensated with an increasing of the Petzval curvature, so a limit on this aberration has been necessary. This limit has been fixed at 0.05mm.

The smaller value for distortion we get is **–2.18mm**, but this final result has been reached with very fine adjustments of the value obtained from simply imposing required condition on aberration.

To have an idea about distortion influence on image quality we consider the best value and a different values close to it, we obtained in the process of optimization, reminding that we deal with only a single direction, the baseline one, keeping results valid for the whole FOV by circular symmetry. Let's indicate distortion with DIST:

A) DIST = -3.00 mm
B) DIST = -2.18 mm

NOTE : it could be argumented about the fact that, having the distortion a negative sign, the optimisation goes through greater value. Nevertheless in aberration theory the sign means only the versus on which a certain aberration acts as regards the ideal focal plane. The absolute value has significance to indicate the real amount.

CASE A)

Ray aberration term	Ray aberration value in mm between ideal and real focal points as function of the distance from the centre field					
	0.0 deg	**0.1 deg**	**0.2 deg**	**0.3 deg**	**0.4 deg**	**0.5 deg**
Spherical			0.004			
Tan. coma	0.000	0.004	0.008	0.013	0.016	0.021
Tan. Astigmatism	0.000	0.001	0.002	0.006	0.010	0.016
Sag. Astigmatism	0.000	0.002	0.002	0.004	0.007	0.012
Petzval	0.000	0.002	0.002	0.004	0.006	0.010
Distortion	0.000	-0.023	-0.192	-0.648	-1.536	**-3.000**

The geometrical layout has this configuration:

Radii of Curvature (mm) Conic constant (K)		**Mirror Separation (mm)**	
M1	-6475.86	M1-M2	-2714.03
K1	-0.99		
M2	-1286.81	M2-M3	2895.54
K2	-2.04		
M3	flat	M3-M4	986.21
M4	1611.40	M4-M5	1386.21
K4	-0.71		
M5	flat	M5-FP	1961.22

This new geometry gives a greater distance between M3 and M4 and a removal of the focal plane away from M5, but this last consequence is no so important being M5 a flat mirror.

More interesting is the fact that now we have a geometric location of M3, M4, M5 and of the apertures of the system about on the same plane. This can gives the opportunity to assembly these elements on the same bench.

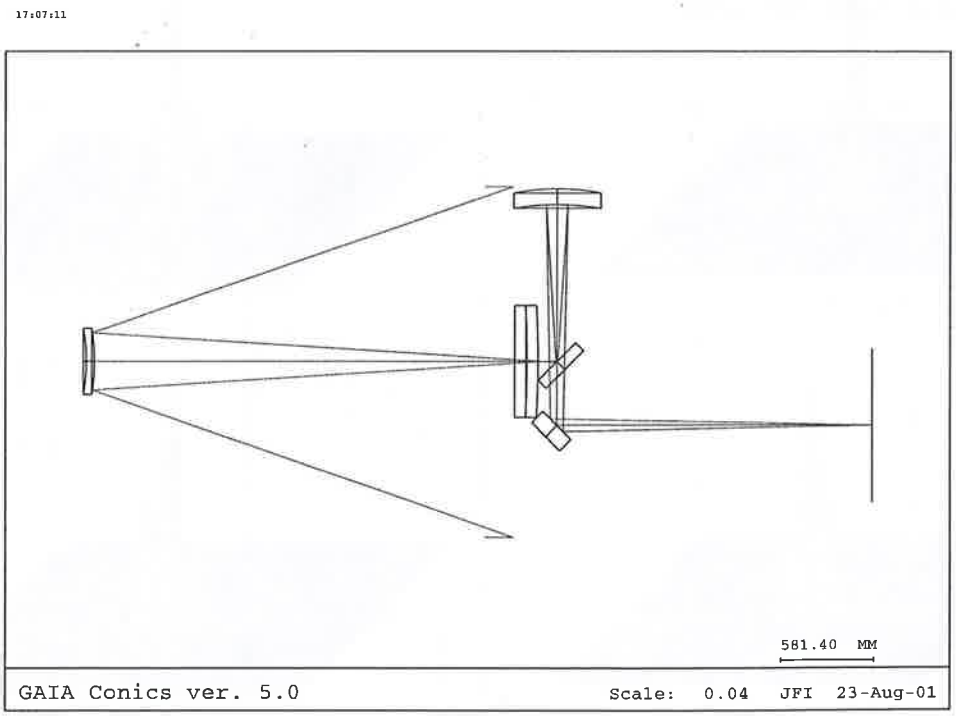

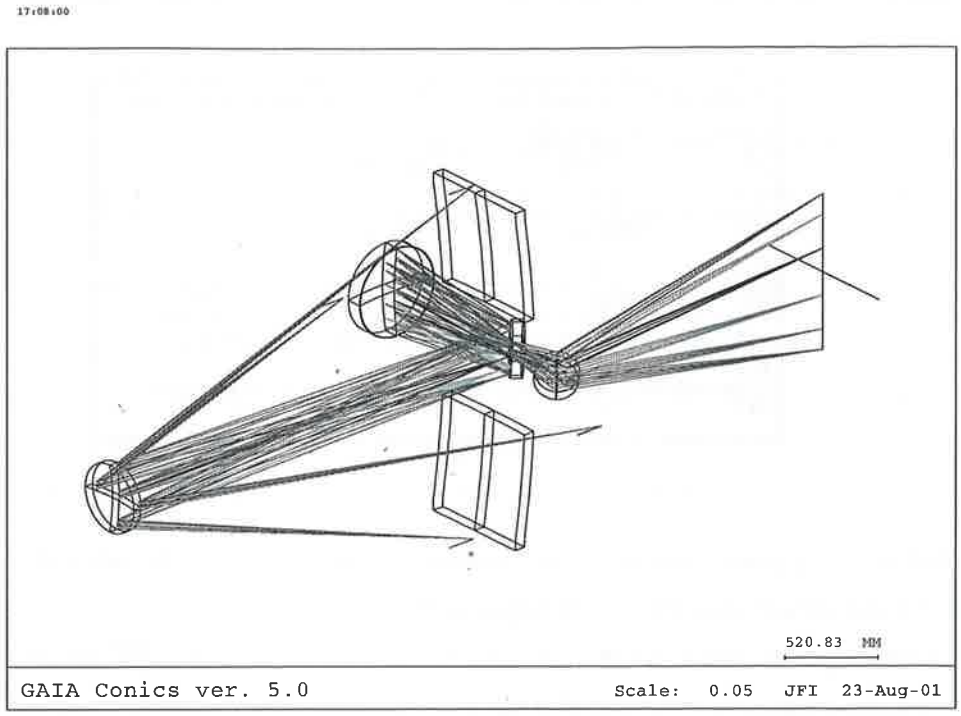

With this new configuration we got a little enlargement of the pupil on M3 but a significant improvement of the PSFs quality.

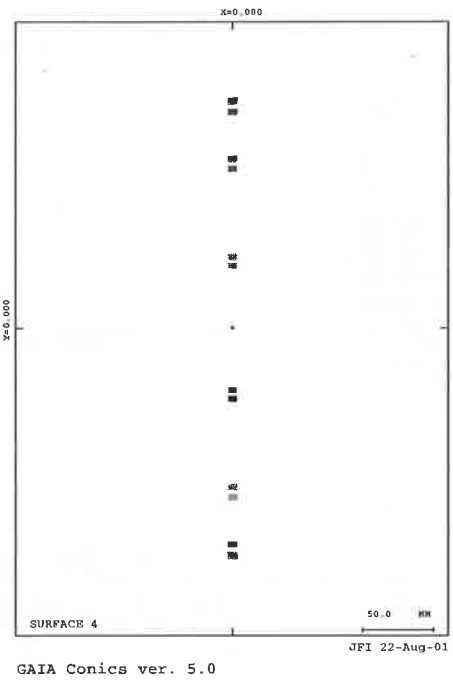

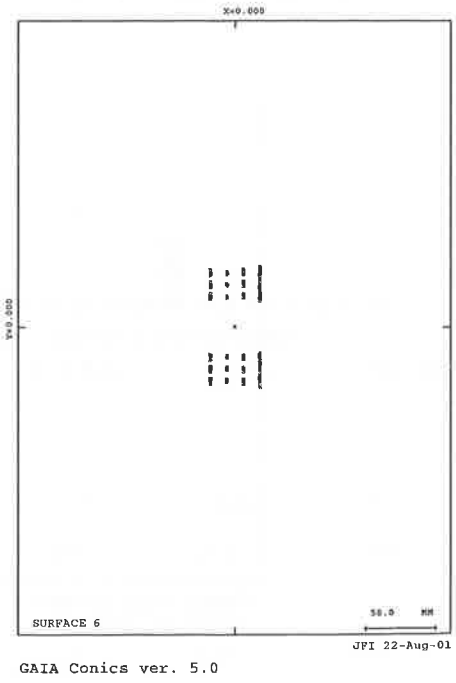

In the following, point spread functions along the high-resolution direction are grouped.

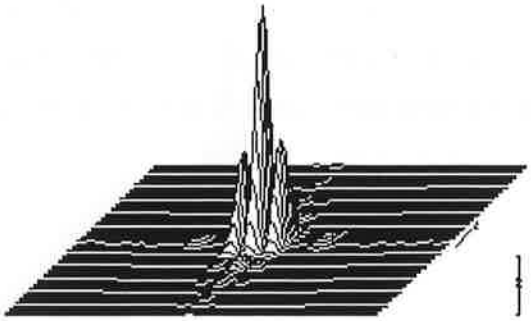

PSF at (0 , 0.15) deg

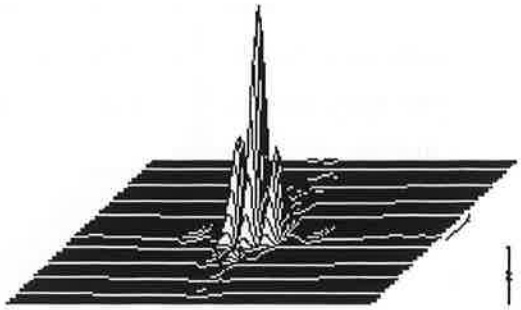

PSF at (0 , -0.15) deg

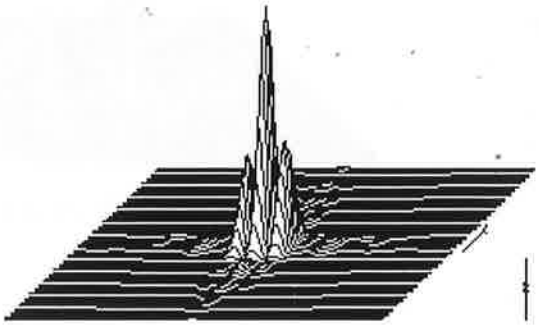

PSF at (0 , 0.25) deg

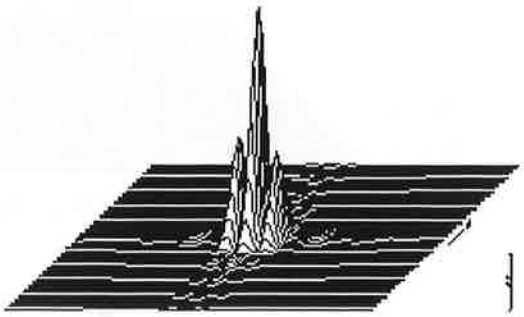

PSF at (0 , -0.25) deg

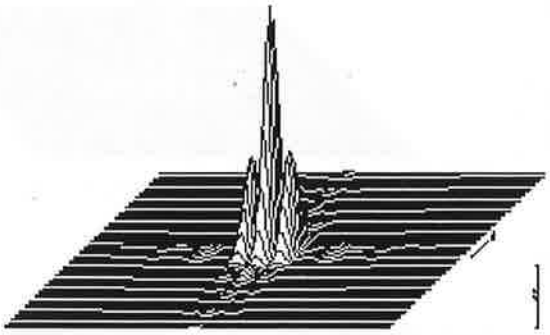

PSF at (0 , 0.37) deg

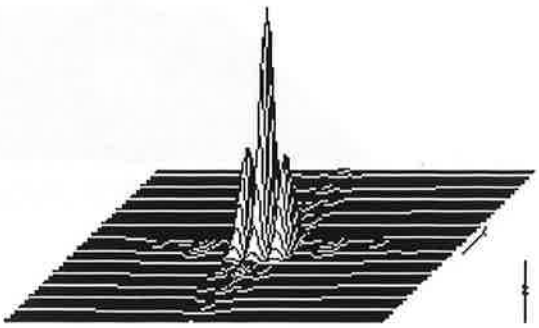

PSF at (0 , -0.37) deg

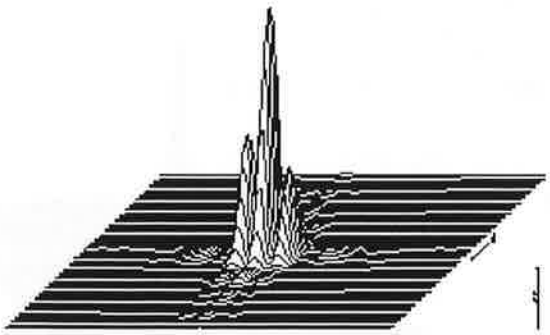

PSF at (0 , 0.50) deg

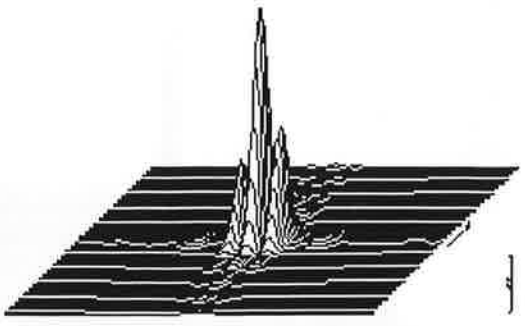

PSF at (0 , -0.50) deg

We report the PSFs for all the fixed points only to put attention on the variation of the symmetry from positive to negative coordinates.

In the following other PSFs are pictured only for the first quadrant, taking into account that points in 1 and 2 quad. have the same PSFs, while those in 3 and 4 quad have the same light distribution but with the PSF lobes inverted. We check the quality considering the same points along X, at Y=0: (0.15,0), (0.25,0) ,(0.37,0) , (0.5,0)

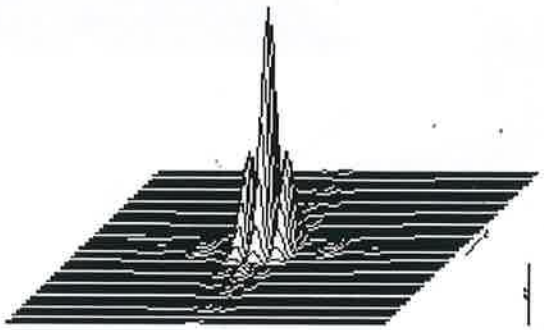

PSF at (0.15 , 0)deg

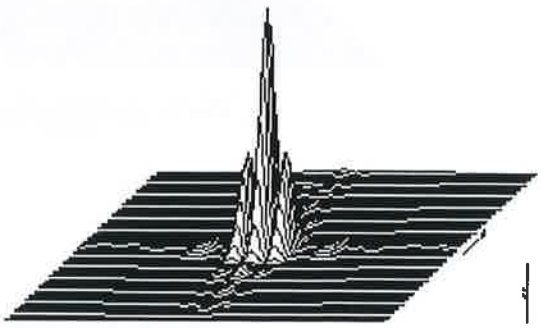

PSF at (0.25 , 0) deg

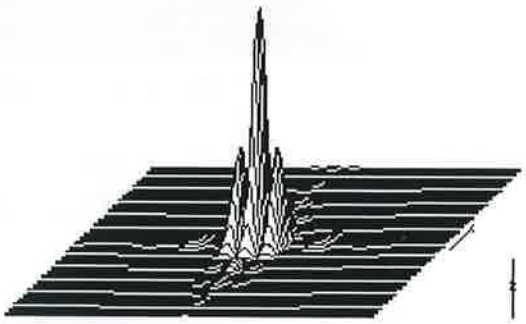

PSF at (0.37 , 0)deg

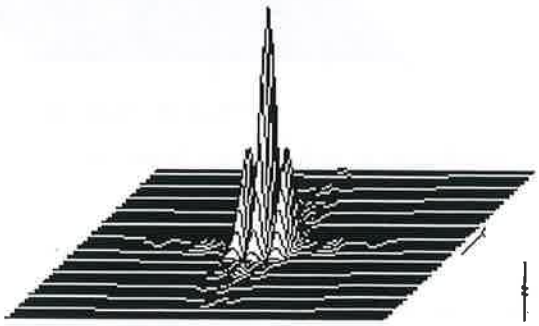

PSF at (0.5 , 0) deg

Besides, other 4 points in the first quadrant has been fixed: (0.2,0.2) , (0.35,0.35) , (0.2,0.35), (0.35,0.2)

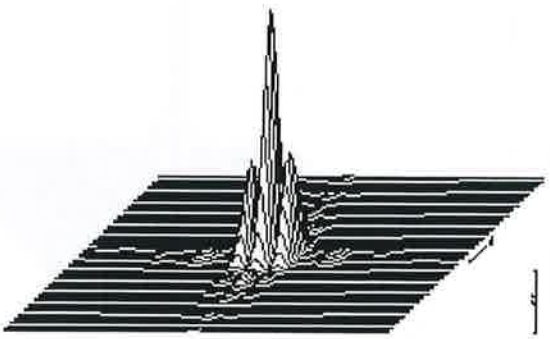

PSF at (0.2 , 0.2) deg

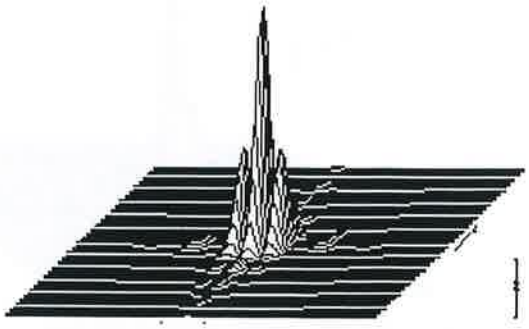

PSF at (0.2 , 0.35) deg

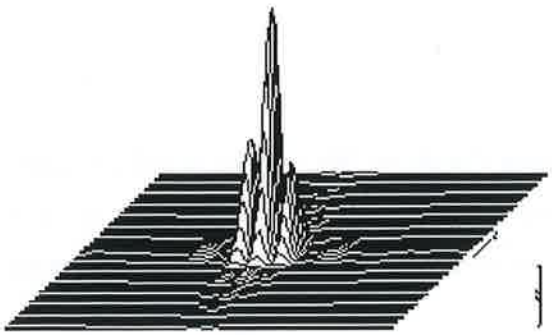

PSF at (0.35 , 0.35) deg

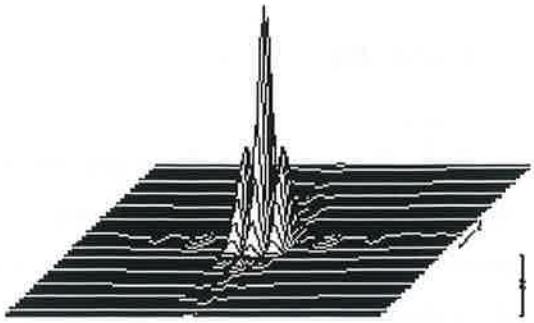

PSF at (0.35 , 0.2) deg

The choice of these points is about arbitrary but 0.35 is not so casual because is exactly 0.5/(sqrt2), so to have a total field of 0.7x0.7 deg.

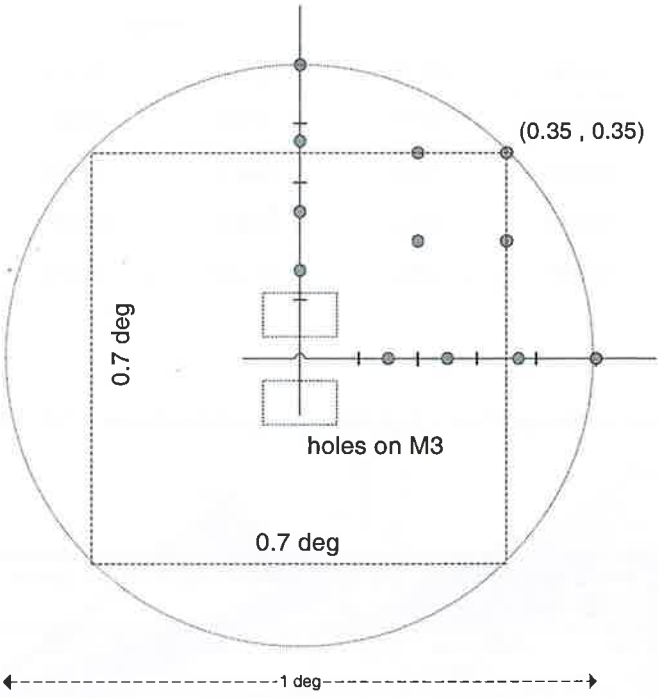

Fig. 5 Field of View – FOV – considered for the optimization

CASE B)

Fine adjustments have been performed starting from CASE A). We wanted to reduce further the distortion, bounding the *comatic* aberration to the lower value of 0.02 (we check that this is the lowest possible value), relaxing a little the requirements on exit pupil dimensions. We discuss in the following how this affects light distribution on the Focal Plane

The results we got are very good. The distortion can be corrected till –2.18 with a little enlargement of the pupils on M3 that can be accepted if compared to the improved image quality.

Ray aberration term	**Ray aberration value in mm between ideal and real focal points as function of the distance from the centre field**					
	0.0 deg	**0.1 deg**	**0.2 deg**	**0.3 deg**	**0.4 deg**	**0.5 deg**
Spherical			0.008			
Tan. coma	0.000	0.005	0.010	0.015	0.020	0.025
Tan. Astigmatism	0.000	0.001	0.003	0.007	0.013	0.021
Sag. Astigmatism	0.000	0.000	0.001	0.002	0.004	0.006
Petzval	0.000	0.000	0.000	0.000	0.000	-0.001
Distortion	0.000	-0.017	-0.139	-0.471	-1.118	**-2.184**

The geometry is about unchanged but a little increasing of the distance M5-FP. The footprint shows the slightly enlarged pupil.

Radii of Curvature (mm) Conic constant (K)		**Mirror Separation (mm)**	
M1	-6480.04	M1-M2	-2726.94
K1	-0.99		
M2	-1292.25	M2-M3	2521.84
K2	-2.21		
M3	flat	M3-M4	-1007.54
M4	1565.43	M4-M5	1407.54
K4	-0.70		
M5	flat	M5-FP	2219.57

11:14:38

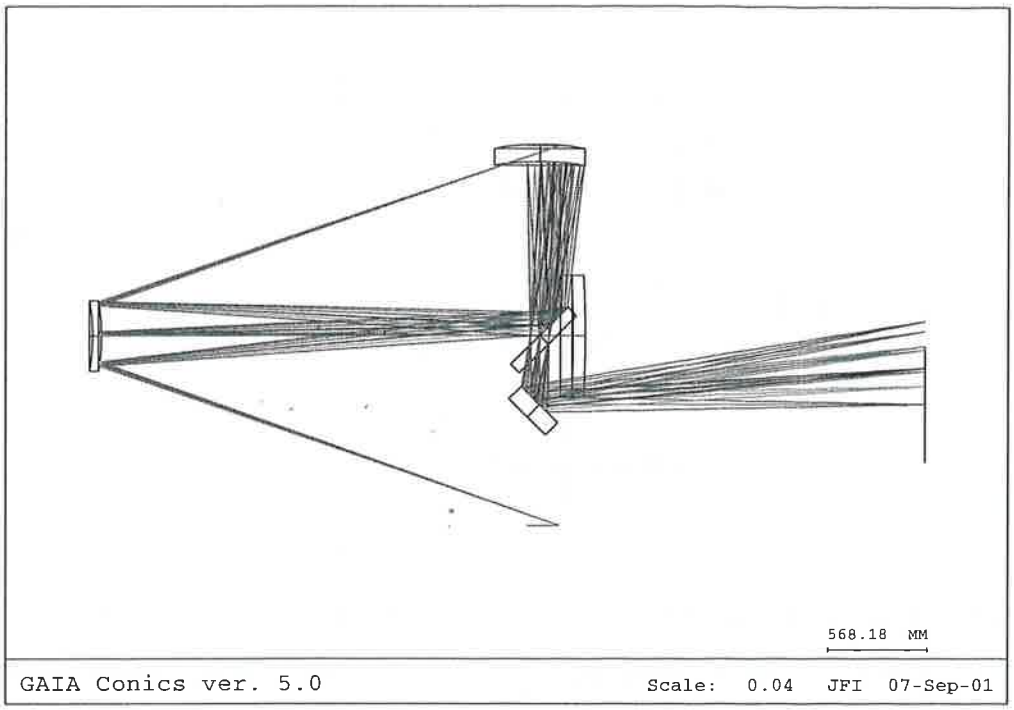

11:15:23

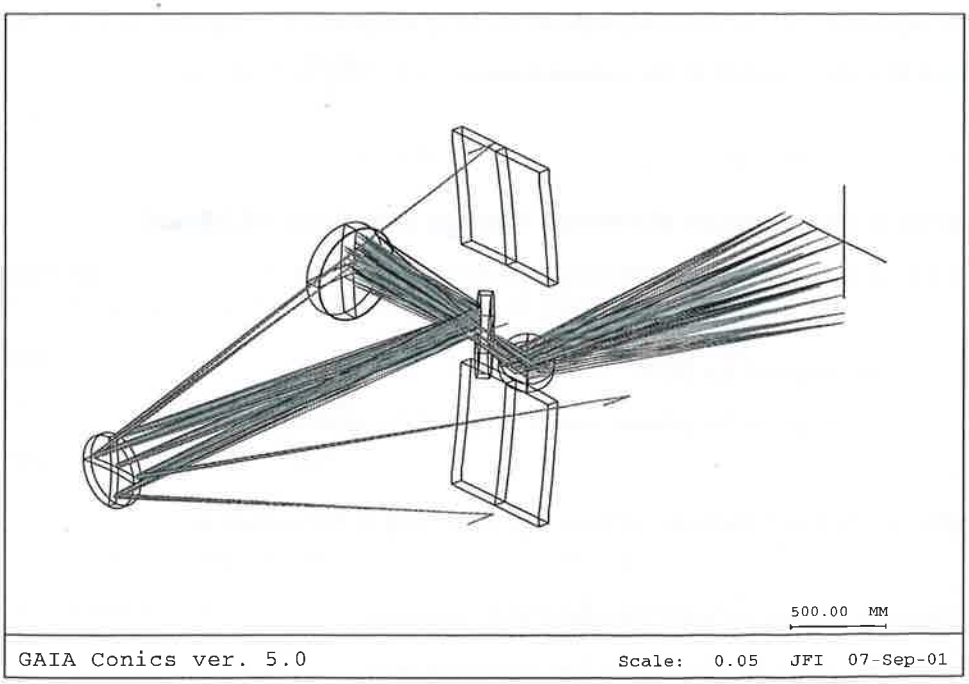

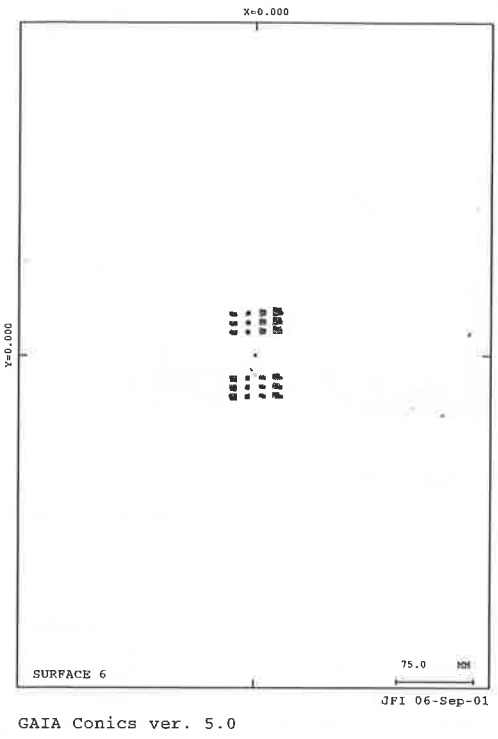

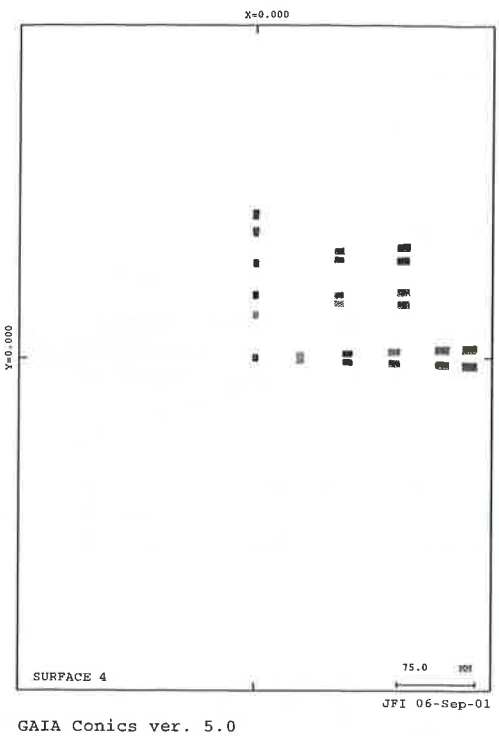

These footprints have not the same scale of the footprint previously reported but, to compare, it must be accounted that the first field in the vertical direction is 0.15deg in both cases.

5. Clipping of the beam on M3 mirror (design with dist= –2.18mm)

The optical design is such that at the height of the tertiary mirror (M3) are positioned both

a) an image of the FOV

b) an image of the primary mirror (pupil of the system)

Geometry is as follows: the scale of the image (a) at level of M3 surface is

~284 mm/ degree on the Y axis (high resolution one)

~422 mm/ degree on the X axis (low resolution one)

the different scaling is due to the fact that M3 is oriented 45° with respect to the beam.

Geometry of the clipped area is as in figure. Dimensions are derived from ray-tracing:

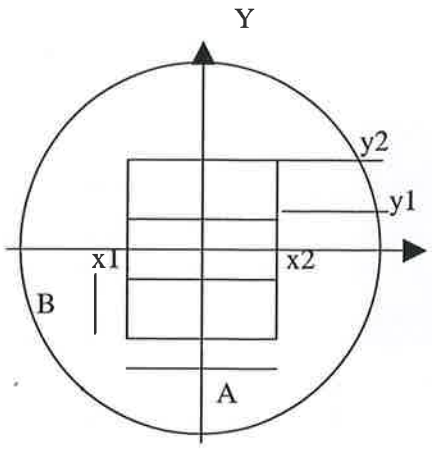

Fig. 6 Exit pupil on M3

We can assume as clipping area ON M3 SURFACE a couple of rectangle defined by the coordinates (with respect to the centre of the mirror):

rect. 1	x1: -23 mm	x2: 26 mm	y2: 46 mm	y1: 20 mm
rect. 2	x1: -23 mm	x2: 26 mm	y2: -46 mm	y1 -20 mm

scaling to degrees on the image this means:

rect. 1	left: -0.059	right: 0.063	top: 0.165	bottom: 0.072
rect. 2	id.			

dimensions of the rectangle is: A = ~49 mm , B = ~ 26 mm, this means, on the Focal Plane (scale is 1 degree = 966mm)

A ~ 0.122 deg.	~ 118 mm
B ~ 0.093 deg	~ 90 mm

Gap between the two rectangles is about:	2 * y1 ~ 0.144 deg	~ 139 mm
Total fraction of area lost is:	0.02 sq deg / 0.5 sq deg	= 4%

It should be verified that this percentage of lost field remains the same for dist = -3mm and dist = -2.18mm too.

Following figure shows a possible disposition for the 30x60 mm CCDs (gray = uncovered area)

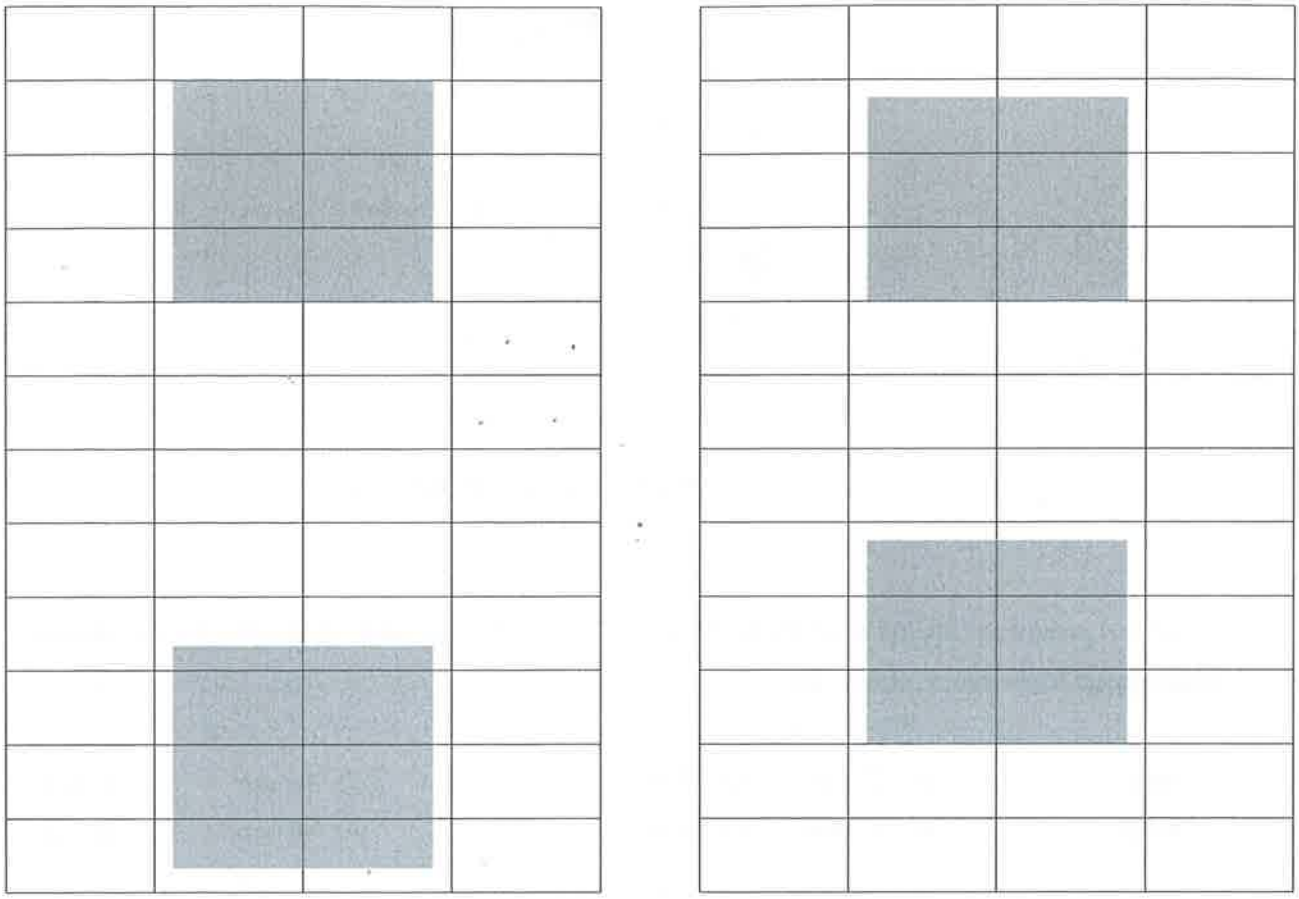

Fig. 7 Projection on the CCD array in the focal plane of the holed area

This scheme gives a sketch of the number of CCD shadowed by the holes on M3. Each white rectangle is a 30mm x 60mm CCD, while the grey one are the projected holes on the FP. The left array is that we could foreseen for the case with dist = -2.18mm, the right on that with dist = -3mm.

In the following pages, we report tables and plots of distortion. It is possible to compare results to have a direct feedback of the improved performances.

As still underlined, the values reported in tables are the differences between the radial position, referred to the optical axis, of the focal point of a real ray and the corresponding ideal focal point of a ray with no aberration normalised to the ideal radial distance and expresses in percentage of the normalization term

CASE A)

	Distortion (%)										
(degrees)											
-0.5	1.25	1.02	0.84	0.72	0.64	0.62	0.64	0.72	0.84	1.02	1.25
-0.4	1.02	0.79	0.62	0.49	0.42	0.39	0.42	0.49	0.62	0.79	1.02
-0.3	0.84	0.62	0.44	0.32	0.24	0.22	0.24	0.32	0.44	0.62	0.84
-0.2	0.72	0.49	0.32	0.19	0.12	0.09	0.12	0.19	0.32	0.49	0.72
-0.1	0.64	0.42	0.24	0.12	0.04	0.02	0.04	0.12	0.24	0.42	0.64
0.0	0.62	0.39	0.22	0.09	0.02	0.00	0.02	0.09	0.22	0.39	0.62
0.1	0.64	0.42	0.24	0.12	0.04	0.02	0.04	0.12	0.24	0.42	0.64
0.2	0.72	0.49	0.32	0.19	0.12	0.09	0.12	0.19	0.32	0.49	0.72
0.3	0.84	0.62	0.44	0.32	0.24	0.22	0.24	0.32	0.44	0.62	0.84
0.4	1.02	0.79	0.62	0.49	0.42	0.39	0.42	0.49	0.62	0.79	1.02
0.5	1.25	1.02	0.84	0.72	0.64	0.62	0.64	0.72	0.84	1.02	1.25
	-0.5	-0.4	-0.3	-0.2	-0.1	0.0	0.1	0.2	0.3	0.4	0.5
	(degrees)										

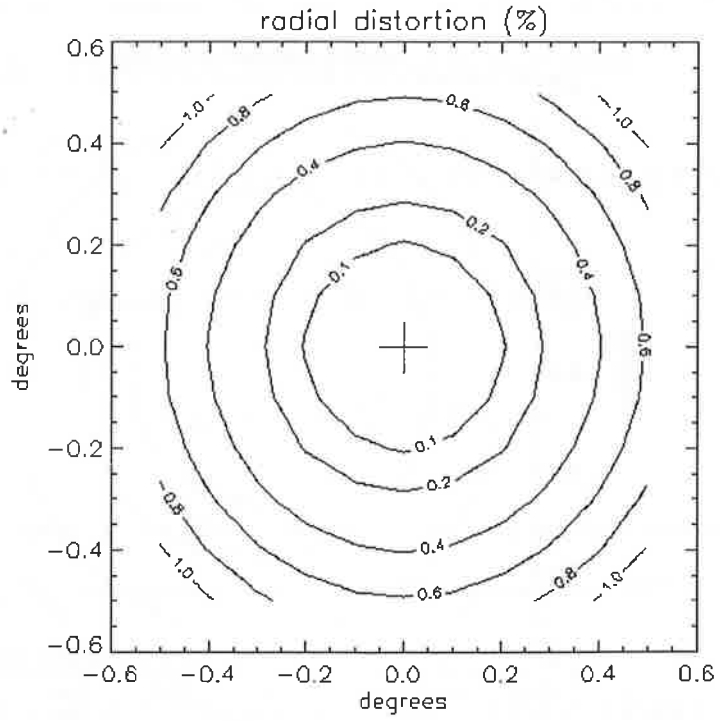

CASE B)

	Distortion (%)										
(degrees)											
-0.5	0.90	0.74	0.61	0.52	0.46	0.44	0.46	0.52	0.61	0.74	0.90
-0.4	0.74	0.57	0.44	0.35	0.30	0.28	0.30	0.35	0.44	0.57	0.74
-0.3	0.61	0.44	0.32	0.23	0.17	0.15	0.17	0.23	0.32	0.44	0.61
-0.2	0.52	0.35	0.23	0.14	0.08	0.06	0.08	0.14	0.23	0.35	0.52
-0.1	0.46	0.30	0.17	0.08	0.03	0.01	0.03	0.08	0.17	0.30	0.46
0.0	0.44	0.28	0.15	0.06	0.01	0.00	0.01	0.06	0.15	0.28	0.44
0.1	0.46	0.30	0.17	0.08	0.03	0.01	0.03	0.08	0.17	0.30	0.46
0.2	0.52	0.35	0.23	0.14	0.08	0.06	0.08	0.14	0.23	0.35	0.52
0.3	0.61	0.44	0.32	0.23	0.17	0.15	0.17	0.23	0.32	0.44	0.61
0.4	0.74	0.57	0.44	0.35	0.30	0.28	0.30	0.35	0.44	0.57	0.74
0.5	0.90	0.74	0.61	0.52	0.46	0.44	0.46	0.52	0.61	0.74	0.90
	-0.5	-0.4	-0.3	-0.2	-0.1	0.0	0.1	0.2	0.3	0.4	0.5
	(degrees)										

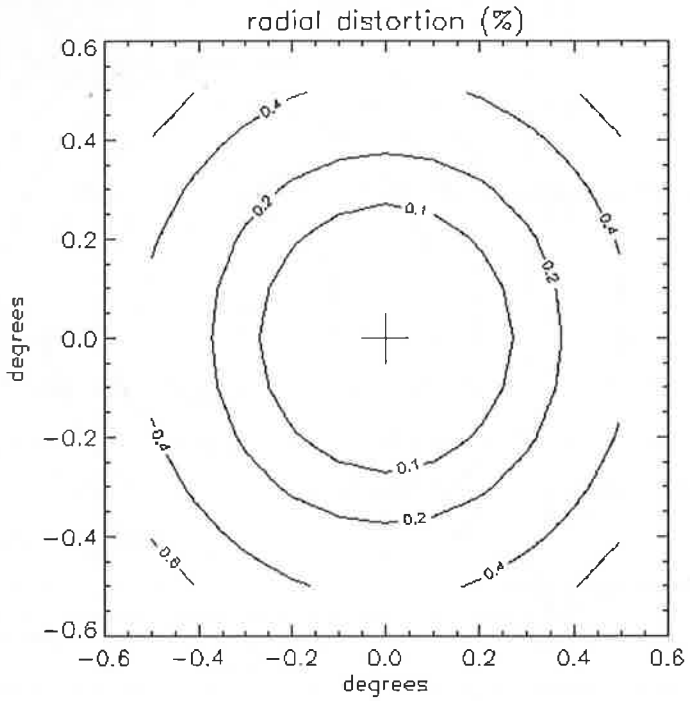

As still remarked previously, if we consider a section along Y-axis of the distortion distribution, we can compare the trend of both cases.

6. Distortion and CCD time clocking

The target movement on the sky is at constant speed, associated to the satellite rotation speed $V_s = 120''/s$; the apparent speed on the focal plane is variable, due to the distortion. The *optical scale* $s = 1/F$ (reciprocal of the effective focal length) is the nominal value of conversion factor between object plane and image plane, constant in the ideal case. Distortion corresponds to a locally variable scale. For the new interferometric configuration of GAIA, $F = 55m$ and $s = 3.75''/s$.

Code V provides an estimate of local distortion as the linear distance δx on the focal plane between the paraxial image (ideal system) placed at position x and the actual diffraction image (real system) at $x + d$. The position η on the sky is then associated to the nominal position $x = F\eta$ and to the effective position $x' = x + d = F\eta + d$. The evolution of the position on the sky is $\eta(t) = \eta_0 + V_s \cdot t$; then, the nominal speed on the focal plane is $\dot{x} = F\dot{\eta} = FV_s = V_f$.

Distortion in a centred system is usually negligible on the optical axis, i.e. in a central region of the focal plane (paraxial approximation), and progressively increasing with the distance from the centre (e.g. radially). We can consider a polynomial expansion of the distortion, limited to the second order: $d = D \cdot x^2$. Under normal conditions, the distortion is small: $x \approx x'$, i.e. $d \ll x$, and $x' = F\eta + DF^2\eta^2$. The apparent motion on the focal plane of the target is then

$$x' = F \cdot (\eta_0 + V_s t) + DF^2(\eta_0 + V_s t)^2 = F\eta_0 + FV_s t + DF^2\eta_0^2 + 2DF\eta_0 FV_s t + DF^2 V_s^2 t^2$$

which becomes, using the notation $x_0 = F\eta_0$ and $x_0' = F\eta_0 + DF^2\eta_0^2$:

$$x' = x_0' + V_f t(1 + 2Dx_0) + DV_f^2 t^2.$$

The constant rotation speed on the object plane is mapped as a *variable* speed on the focal plane: $\dot{x}' = V_f(1 + 2Dx) + 2DV_f^2 t$, corresponding to a constant acceleration: $\ddot{x}' = 2DV_f^2$. At first order, in the expression above, we can replace x with x'.

The baseline GAIA CCD has $N = 2780$ columns of pixels with size $P = 9\,\mu m = 33.75\,mas$ along the high-resolution direction, for a total length $L = 25\,mm = 94'' \cong 1'.5$, corresponding to an elementary TDI exposure time $T_{TDI} = L/V_s = 0.783\,s$. The nominal clock rate must match the sidereal speed: the pixel cycle time is $T_P = P/V_s = 0.28\,ms$, corresponding to $1/T_P = 3.56\,klines/s$. Since the scan speed is constant over the chip, it can be matched only at a single point, e.g. the mid section of the device:

$$V_f^{mean}([x_0', x_0'+L]) = V_f \cdot [1 + 2D(x_0'+L/2)].$$

The elementary exposure duration T, i.e. over the chip length $\Delta x' = L$, from x_0' to $x_0'+L$, is approximately $T = T_0(1-2Dx')$, where $T_0 = L/V_f = sL/V_s$ is the nominal exposure period, valid in the central region of the focal plane.

A requirement on the distortion may be set in order to have a mismatch between the CCD clocking (charge image) and the photon image of no more than a fraction of pixel over the whole device. The speed is matched at the CCD centre, so that the speed mismatch is

$$\Delta V = \dot{x}' - V_f^{mean} = V_f \cdot [1 + 2Dx_0 + 2DV_f t - 1 - 2Dx_0' - 2DL/2] = 2DV_f(V_f t - L/2)$$

Integrated over the first half of the exposure, it results in a relative image displacement

$$\Delta x' = \int_0^{T/2} \Delta V dt = 2DV_f \int_0^{T/2} (V_f t - L/2) dt = \ldots = -DL^2/4$$

In particular, if we require a displacement not larger than 1/3 pixel, i.e. $3\,\mu m$, then the requirement on the distortion parameter is $|D| \le \frac{4\Delta s}{L^2} \cong 2 \cdot 10^{-5}\, mm^{-1}$.

At the border of the field we consider $x \cong 480\,mm$, $|x'-x|_A \cong 2.18\,mm$ and $|x'-x|_B \cong 3.00\,mm$, so that $D_A \cong 1.3 \cdot 10^{-5}\, mm^{-1}$ and $D_B \cong 0.9 \cdot 10^{-5}\, mm^{-1}$. For both configurations the requirement is satisfied.

The correspondent image displacement on the CCD is of about $\Delta x_A' \cong 2\,\mu m \cong 1/4\, pixel$ and $\Delta x_B' \cong 1.4\,\mu m \cong 1/6\, pixel$

The image scale variation can be expressed in terms of the variation of the separation between corresponding points, respectively in object plane ($\Delta\eta = \eta_2 - \eta_1$) and image plane

$$\Delta x' = x_2' - x_1' = \Delta x + 2Dx\Delta x = \Delta x(1 + 2Dx) = (F + \Delta F)\Delta\eta,$$

where $x = (x_1 + x_2)/2$, so that $\Delta F = 2DFx$.

With the above values, the scale variation between a point on the optical axis and a point at the border of the FOV is $(\Delta F/F)_A = 1.2\cdot 10^{-2}$ (case A) and $(\Delta F/F)_B = 0.9\cdot 10^{-2}$ (case B); both results are lower than the target design value, which is $(\Delta F/F) = 1.9\cdot 10^{-2}$.

This kind of calculation is valid only for local value of the distortion and we could expect the same value for all the point on the axis, if the approximation to a parabola we assume at the beginning, was exact.

This is not the case. One can verify that point calculation performed for other values of x gives different estimation of D; nevertheless, result obtained for x – 480mm is an upper limit. As a further check, one can perform a parabolic fit on all the distortion value for a fixed axis.

We verify this point and the output is pictured in the following figure.

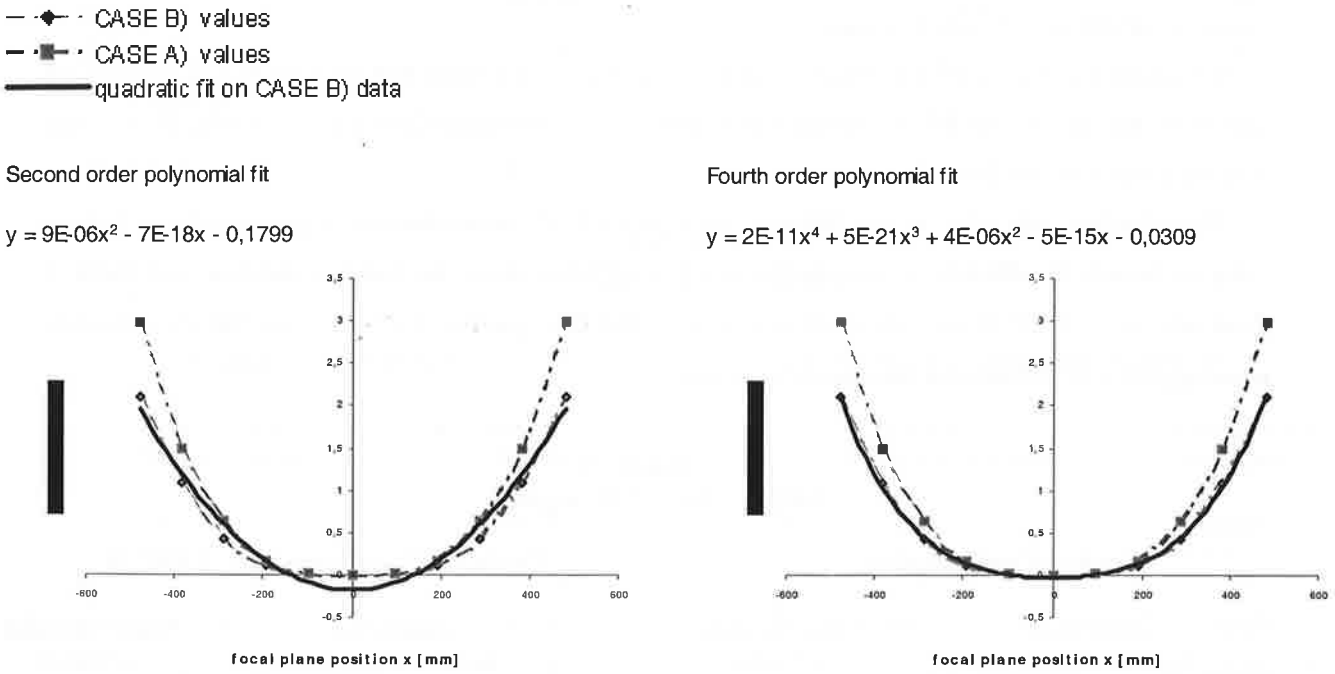

Fig. 8 Polynomial fit for the data obtained in the optimization proces

In the second order fit, the coefficient of x^2 is equal to the value of D we calculated that confirms a good agreement between the analytical treatment and the empirical data. In any case, assuming parabolic behaviour for distortion is restrictive and, as it can be seen in the right figure, a fourth order fit gives a better approximation of the data trend. This point could be argument of future widening.

7. Discussion of Aberrations in terms of Zernike Polynomials

The same discussion can be accomplished in terms of Zernike polynomials. Up to now we presented the results of optical system performances estimation for GAIA considering the ray aberrations at the focal plane. Improvements have been connected to the reduction of the ray aberration as more as possible that means substantially the reduction of the spot diagram.

We underlined that GAIA interferometer scheme can be assumed as circular symmetric and so the Seidel Coefficients are a good mean to check the optimisation progresses. A similar treatment could be developed using Zernike coefficients as indicators of optical performances changes, with the only difference that now a map of the wavefront at the exit pupil can be detailed.

This approach doesn't base on the geometrical parameters of the system for calculations but refers to the wavefront itself as an analytical function that is approximated with a polynomial series by means of the Least Square Method. Coefficients of the polynomials that fit better the wavefront function are the indicators of amount of each aberration.

We report a summary of the results we got for Zernike polynomials with CODE V and the map of each term for the current Bakup Configuration and for our Optimised Configuration CASE B), i.e. that with the lower value of Seidel Distortion.

The following table refers to two different points in the FOV we considered; in particular Table 1 gives value of Zernike Coefficient on axis, Table 2 at (0.0 , 0.5)deg, along the baseline direction and Table 3 gives value at (0.35 , 0.35)deg.; the outermost point in the first quadrant. In both cases only the reference wavelength λ = 0.750 microns has been considered.

Table 1

Field (0.0 , 0.0) degrees

Backup Configuration			Optimized configuration CASE B		
	Aberration Zernike Coefficient	Value (lambda) at 750nm		Aberration Zernike Coefficient	Value (lambda) at 750nm
Z1	piston	-0.0620	Z1	piston	-0.0191
Z2	tangential tilt	0.0000	Z2	tangential tilt	0.0000
Z3	sagittal tilt	0.0000	Z3	sagittal tilt	0.0000
Z4	tangential astigmatism	0.1138	Z4	tangential astigmatism	0.0000
Z5	sagittal astigmatism	0.0000	Z5	sagittal stigmatism	0.0000
Z6	defocus	0.0288	Z6	defocus	-0.0106
Z7	tangential coma	0.0000	Z7	tangential coma	0.0000
Z8	sagittal coma	0.0000	Z8	sagittal coma	0.0000
Z9	spherical	0.0729	Z9	spherical	0.0083

Table 2

Field (0.00 , 0.50) degrees

	Backup Configuration		Optimized configuration CASE B	
	Aberration Zernike Coefficient	Value (lambda) at 750nm	Aberration Zernike Coefficient	Value (lambda) at 750nm
Z1	piston	0.2108	piston	0.0048
Z2	tangential tilt	0.0000	tangential tilt	0.0000
Z3	sagittal tilt	0.3931	sagittal tilt	-0.0667
Z4	tangential astigmatism	-0.2324	tangential astigmatism	0.0190
Z5	sagittal astigmatism	0.0000	sagittal stigmatism	0.0000
Z6	defocus	0.2171	defocus	0.0001
Z7	tangential coma	0.0000	tangential coma	0.0000
Z8	sagittal coma	0.2244	sagittal coma	-0.0312
Z9	spherical	-0.0118	spherical	-0.0050

Table 3

Field (0.35 , 0.35) degrees

	Backup Configuration		Optimized configuration CASE B	
	Aberration Zernike Coefficient	Value (lambda) At 750nm	Aberration Zernike Coefficient	Value (lambda) at 750nm
Z1	piston	0.2230	piston	0.0051
Z2	tangential tilt	0.2611	tangential tilt	-0.0441
Z3	sagittal tilt	0.2865	sagittal tilt	-0.0436
Z4	tangential astigmatism	0.1161	tangential astigmatism	0.0000
Z5	sagittal astigmatism	0.3048	sagittal stigmatism	-0.0161
Z6	defocus	0.2410	defocus	0.0007
Z7	tangential coma	0.1509	tangential coma	-0.0207
Z8	sagittal coma	0.1636	sagittal coma	-0.0203
Z9	spherical	-0.0003	spherical	-0.0047

One of the questions we deal with is the verification of the exact meaning of these results. We know that the Zernike polynomials are usually considered with the respective normalization term that is different for each polynomial. CODE V doesn't output specifications about this point, and so some effort has been supported to clarify this issue.

We simulate with *IDL* a wavefront, giving as input a certain amount of known aberration. We obtained a map of this wavefront that have been read with CODE V macro "*ADD.seq*" [5].

Now the calculation of the aberration for this wavefront has been run and the output we got was exactly the quantity of aberration we fix for the wavefront aberration.

This result confirms that the vales in tables are exactly the coefficient of each aberration term in the Zernike series, without the normalization term.

8. Graphical map of each Zernike aberration for both configurations

In this paragraph we present a direct graphical comparison of the Zernike aberrations between the Backup Configuration and our Optimised Configuration.

Plots are based on the previously discussed calculation and, in the case of two component aberration (as astigmatism, coma and tilt), refer to total aberration amount, i.e. the resultant of the summation of tangential and sagittal contribution. The only exception is *piston,* that doesn't have a graphical representation.

Last figures report the total RMS wavefront error that is the resultant error due to all aberrations summed together. The improvements of the performances in our final interferometric scheme appear evident.

1) TILT

Backup Configuration	Optimized Configuration
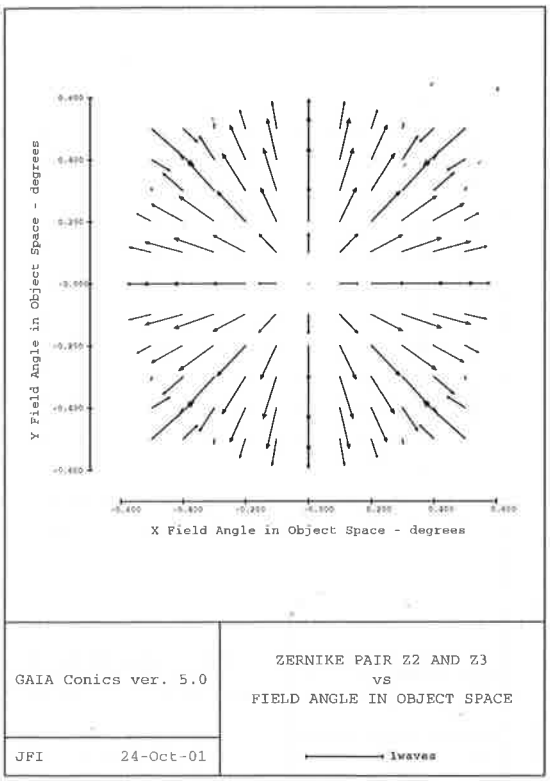	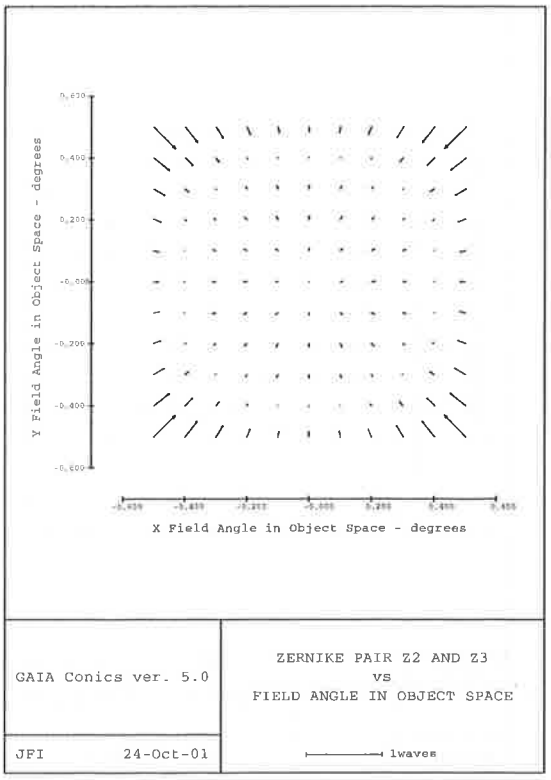

2) ASTIGMATISM

Backup Configuration	Optimized Configuration
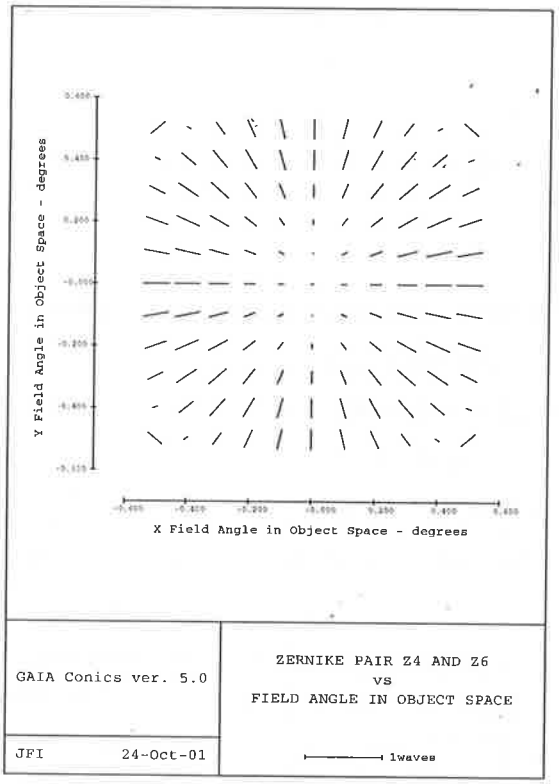	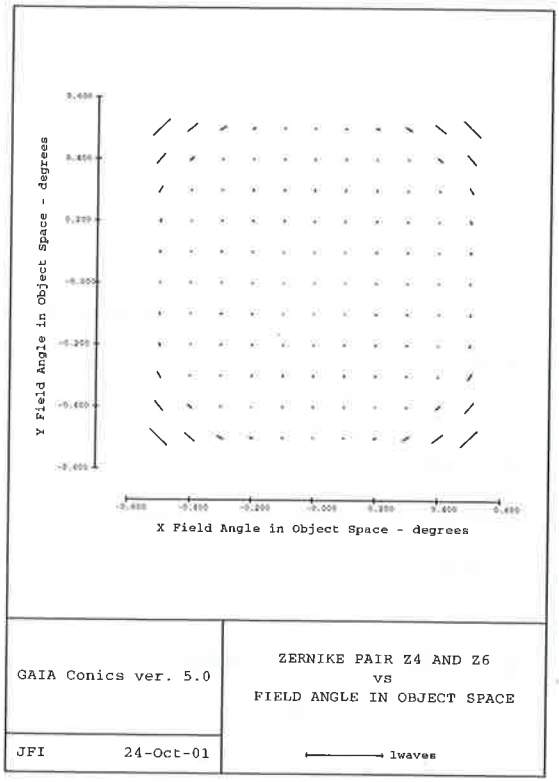

3) DEFOCUS

Backup Configuration	Optimized Configuration
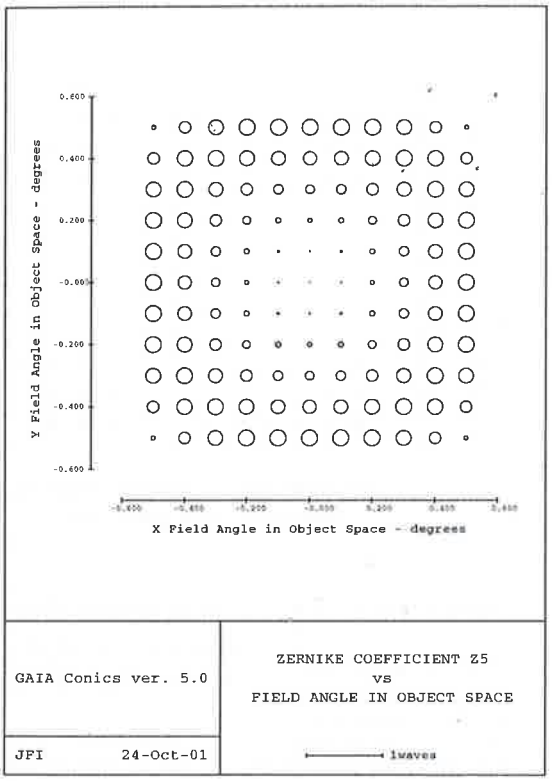	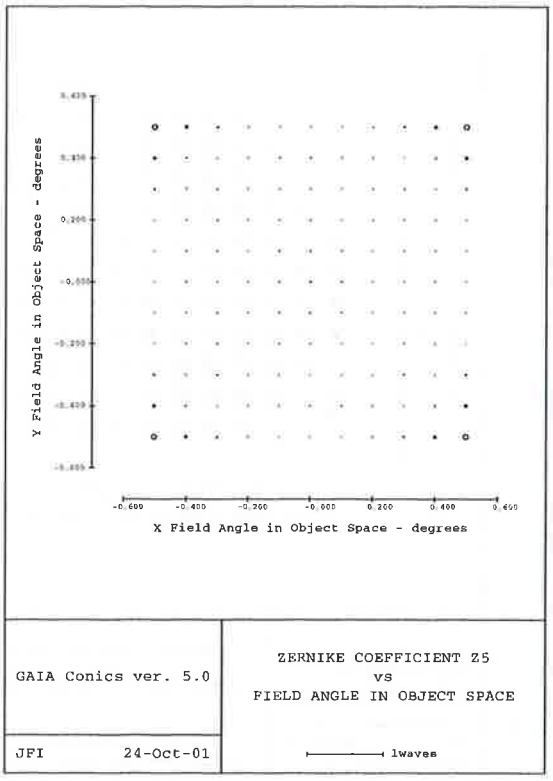

4) COMA

Backup Configuration	Optimized Configuration
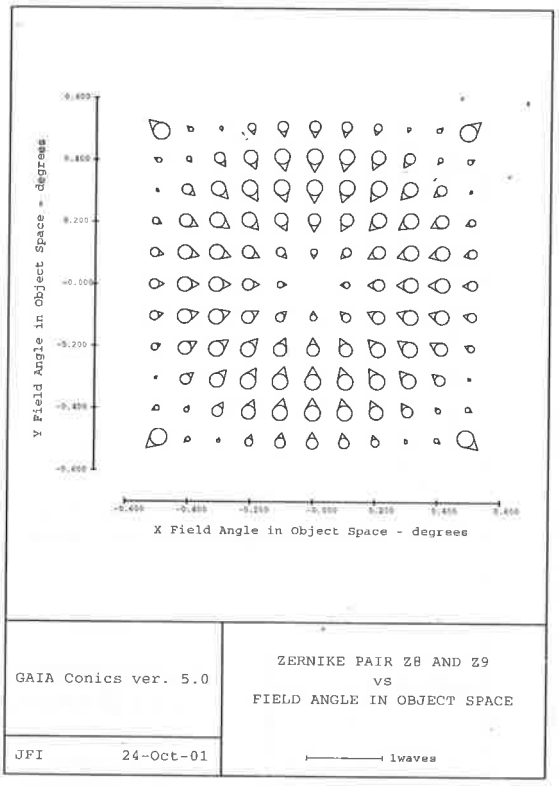	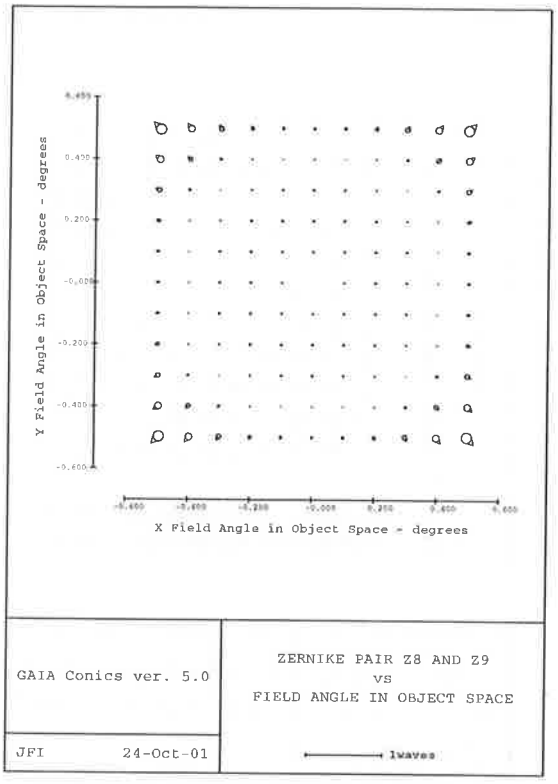

5) SPHERICAL

Backup Configuration	Optimized Configuration
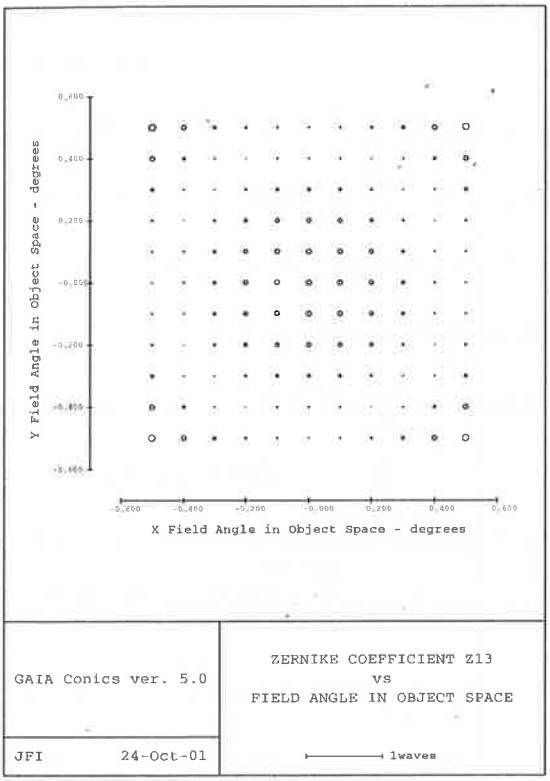	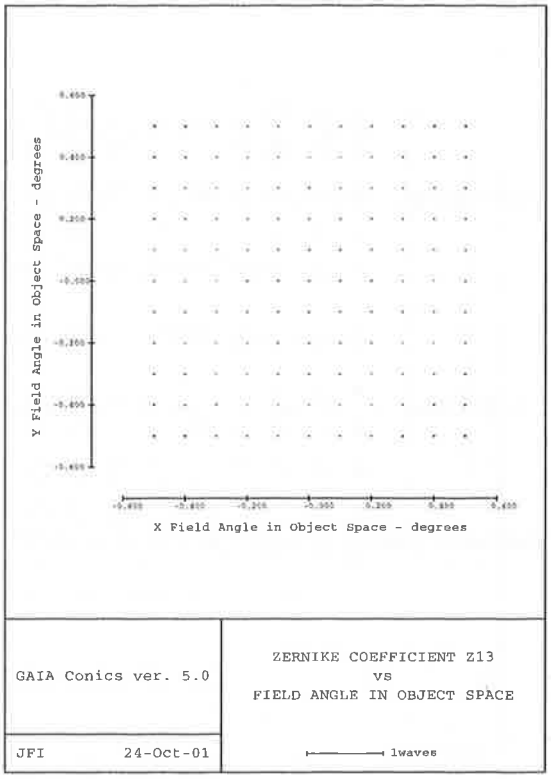

The total RMS wavefront error for the Backup Configuration and for the Optimized Configuration, is :

BackUp Configuration		Optimized Configuration	
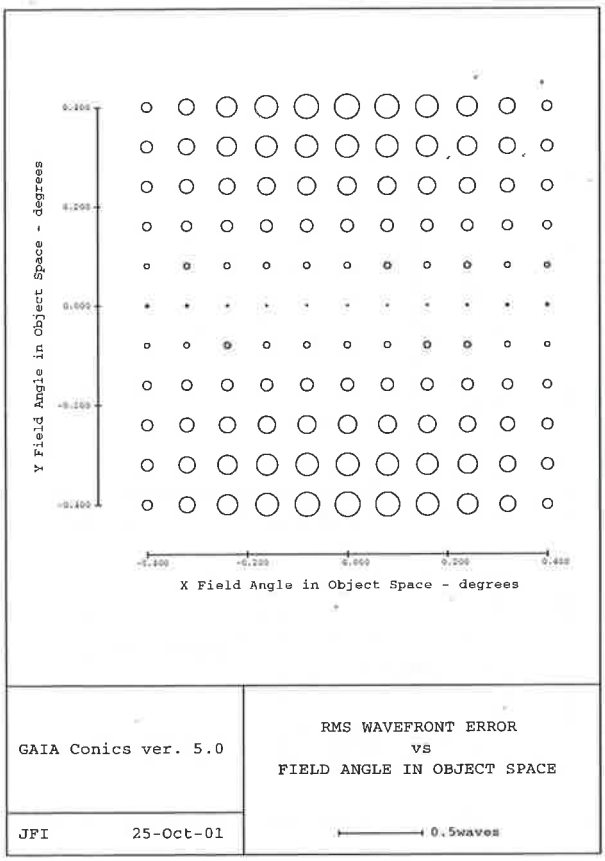		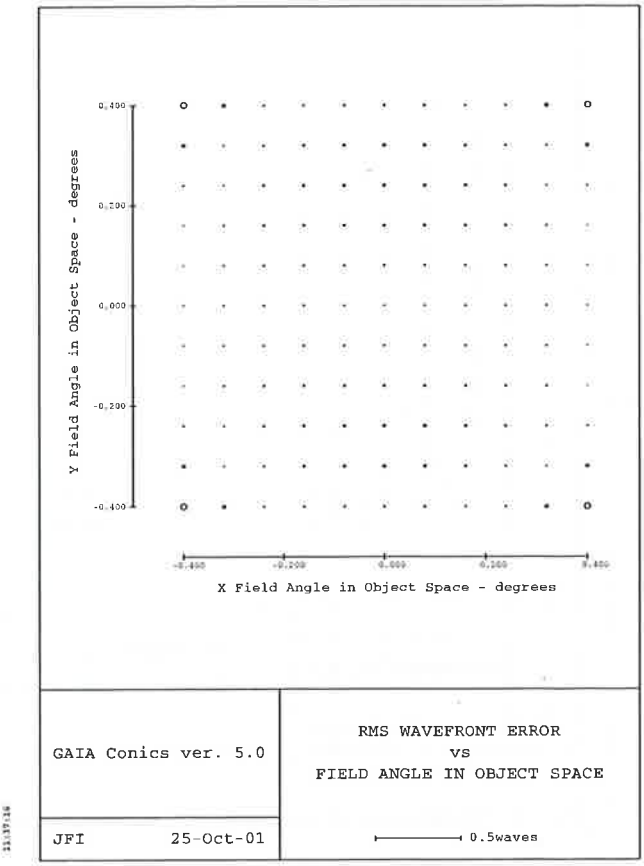	
Maximum value:	0.147	Maximum value:	0.034
Minimum value:	0.007	Minimum value:	0.003
Average value :	0.077	Average value :	0.009
Std deviation:	0.039	Std deviation	0.006

REFERENCES

[1] Gai M. et al, "*An optimized interferometric configuration for GAIA*", August 2001, submitted.

[2] *GAIA PAYLOAD CONFIGURATION* – Alenia Aerospazio Technical Note SD-TN-AI-0544, December 1997

[3] O'SHEA D.C.,"*Elements of Modern optical Design*", John Wiley & Sons, 1985.

[4] Carollo D., Bucciarelli B., Gai M., Lattanti M.G., Ceare S., *"GAIA: global astrometry from space at 10μas level"*, International Cooperation and Technology Transfer.

[5] *CODE V Reference Manual*, Optical Research Associated – ORA, Pasadena.

[6] Rayces J.L., "*Exact relation between wave aberration and ray aberration*", J. Opt. Soc. Am, October 1963.

[7] Mahajan V. N.,"*Aberration Theory Made Simple*", Spie optical Engineering press, Volume TT 6, Donald O'Shea Series Editor, 1991